DYNAMIC STABILITY OF CYLINDRICAL SHELLS BY FINITE ELEMENTS

By

DELVIN ERROL BLACK

Bachelor of Science
Oklahoma State University
Stillwater, Oklahoma
1964

Master of Science
Oklahoma State University
Stillwater, Oklahoma
1965

Submitted to the faculty of the Graduate College
of the Oklahoma State University
in partial fulfillment of the requirements
for the Degree of
DOCTOR OF PHILOSOPHY
May, 1968

DYNAMIC STABILITY OF CYLINDRICAL SHELLS

BY FINITE ELEMENTS

Thesis Approved:

Ahmed Salama
Thesis Adviser

Donald E. Boyd

S. J. McCrary

R. P. Maxwell

N. Durham
Dean of the Graduate College

ACKNOWLEDGMENTS

The author wishes to express his gratitude and sincere appreciation to the following individuals and organizations:

To Professor Ahmed E. Salama for his guidance and friendship throughout the preparation of this thesis;

To Professors Anthony F. Gaudy, Ahmed E. Salama, Donald E. Boyd, and Gordon L. Nelson, members of the advisory committee, for their helpful advice and encouragement;

To the Civil Engineering Department at Oklahoma State University and The National Aeronautics and Space Administration for providing financial assistance for the writer's graduate study;

To the staff of the University Computer Center for their invaluable assistance in the use of their facilities;

To his wife, Verna, for her understanding and encouragement;

To Eldon Hardy for preparing the final sketches;

To Mrs. Donna DeFrain, who typed the manuscript.

Delvin Errol Black

May, 1968

Stillwater, Oklahoma

TABLE OF CONTENTS

LIST OF TABLES

LIST OF FIGURES

LIST OF FIGURES (Continued)

NOMENCLATURE

a	length of an element
$\{a_i\}$	constant matrix
A_i, $\mathring{A}_i$	constants
$\{A\}$, $\{A_a\}$, $\{A_b\}$	matrices of the assumed displacement constants
b	ratio of axial pressure to radial pressure
$[B_a]$, $[B_b]$	constant matrices which relate the assumed displacement constants to the nodal displacements
$\{b_i\}$	constant matrix
c	damping coefficient
d_i	arbitrary displacement
$[d]$	elemental damping matrix
D, $\bar{D}$	flexural and twisting rigidities of the shell
$[D]$	structural damping matrix
E	modulus of elasticity
F_i	damping force
h	shell thickness
$[H]$	matrix relating stress-resultants to strains
i	integer
$[I]$	identity matrix
j	integer

k, $\bar{k}$	in-plane rigidity of the shell; also integer
$[k]$	elemental stiffness matrix
K	curvature
$[K]$	structural stiffness matrix
$[K_{aa}]$, $[K_{ab}]$, $[K_{ba}]$, $[K_{bb}]$	matrices used to express the strain energy of an element
L	length of the shell
$[L]$	matrix used in formulating the stiffness matrix
m	number of half waves in the mode shape along the axis of the shell
$[m]$	elemental mass matrix
$[M]$	structural mass matrix
n	number of sine waves in the mode shape around the circumference of the shell
$\{N\}$	matrix of stress resultants
p	time dependent external pressure
p_o	constant portion of the applied pressure
p_t	magnitude of the time dependent portion of the load
p^*	buckling pressure
$[P]$	matrix used in formulating the stability matrix
$\{q\}$, $\{\dot{q}\}$, $\{\ddot{q}\}$	generalized displacements, velocities, and accelerations
$\{\bar{q}\}$	amplitude of the generalized displacements
$\{Q\}$	generalized forces
$[R]$, $[\bar{R}]$	matrices relating displacement constants and nodal displacements

r	radius of the shell
$[s]$	elemental stability matrix
$[S]$	structural stability matrix
t	time
T	kinetic energy; also the period of the pulsating load
$u, \dot{u}$	axial displacement and velocity
U	strain energy
$v, \dot{v}$	tangential displacement and velocity
V	potential energy of loads
$[V]$	matrix used in formulating the mass matrix
$w, \dot{w}$	radial displacement and velocity
W	the sum of potential and dissipated energy
$\dot{W}$	one-half the time rate at which energy is dissipated by viscous damping
$[W]$	matrix relating strains to assumed displacement constants
x	spatial variable
α	percentage of the buckling pressure which is applied statically
β	percentage of the buckling pressure which is applied as the amplitude of the pulsating portion of the load
γ	slope of the deformed shell along its axis
δ	variational operator
δ_{qj}	virtual displacement
ϵ	strain
$\{\epsilon\}$	strain matrix
η	damping parameter

θ	frequency of applied loads
ν	Poisson's ratio
π	total potential energy
ρ	mass density of the shell material per unit volume
ϕ	spatial variable
ω	natural frequency
Ω	resonant frequency of the shell under constant load
$\{\ \}$	column matrix
$[\ ]$	rectangular matrix
$[\ ]^{-1}$	matrix inverse
$[\ ]^{T}$	matrix transpose

CHAPTER I

INTRODUCTION

1.1 Statement of the Problem

It has been observed both experimentally and analytically that various structures become unstable when subjected to a periodic load, less than the static buckling load, when certain relationships exist between the frequency of the periodic load and the natural frequency of transverse vibrations of the structure. The stability of a thin right circular cylindrical shell subjected to a uniformly distributed axial and radial pulsating pressure is investigated in this thesis. The results of this analysis are presented by giving the principal regions of instability for several loading and support conditions. A region of instability is defined as the spectrum of those points in the load-frequency space which satisfy certain conditions of instability.

The shells in this study are assumed to be homogeneous, isotropic, and initially perfect. The material is linearly elastic and the assumptions of small deflection theory are assumed.

1.2 Historical Review

Melde, in 1859, discovered the phenomenon of parametric resonance in a stretched string with one end attached to a vibrating tuning fork. The first theoretical explanation of this phenomenon was given by Rayleigh (1) in the 1880's. Most of the recent work in the area of

dynamic stability has been done by Russian investigators. A detailed review of the Russian works in this area through 1951 can be found in an article by Beilin and Dzhanelidze (2).

N. M. Beliaev (3), in 1924, examined the problem of dynamic stability of a straight rod hinged at both ends and found the boundaries of the principal region of instability. In 1935, Krylov and Bogoliubov (4) solved the problem of a straight bar with arbitrary support conditions by applying the Galerkin variational method. Bodner (5), Khalilov (6), Einaudi (7), and Ambartsumian and Khachatrian (8) investigated the dynamic stability of plates loaded with compressive in-plane forces. In 1940 Dzhanelidze and Radtsig (9) published a paper solving the problem of dynamic stability of a circular ring subjected to a radial pulsating load.

Markov (10) investigated anisotropic cylindrical shells in 1949 and Bolotin (11) published several papers on the dynamic stability of spherical shells in 1958. Federhofer (12) published a paper on the dynamic stability of cylindrical shells under axial pressure and Bublik and Merkulov (13) studied the dynamic stability of a shell filled with a liquid. The influence of damping on the boundaries of the regions of instability was discussed by Mettler (14) and Naumov (15). Bolotin (16) published a book, Dynamic Stability of Elastic Systems in 1956, which includes most of the work done in this area before that time.

In 1963 Wood and Koval (17) published some experimental results on dynamic stability of cylindrical shells using mylar cylinders for models. Bieniek, Fan, and Lackman (18) applied Galerkin's method to the problem for cylindrical shells. Also, Agamirov and Vol'mir (19) and Vol'mir (20) employed finite deformation theories for solution of

cylindrical shells and panels.

In all of the above works the problem of dynamic stability was either exactly or approximately reduced to one second-order differential equation of the Mathieu-Hill type. Brachkovskii (21) and Bolotin (22) established a class of problems that can be exactly reduced to one second-order differential equation.

The concept of subdividing a structure into various finite elements for analysis is by no means new. The slope deflection method of structural analysis could be classified as a finite element approach. However, the methodology of the finite element technique as it most usefully applies to plates, shells, and compound structures, has been developed only recently. Turner et al (23), in 1956, presented the first significant work in this area. Melosh (24), Best (25), Pian (26), Zienkiewicz and Cheung (27), and Severn and Taylor (28) developed and extended the method, but did not alter the original concept.

Percy et al (29) used a conical frusta for an element in applying the method to static and vibrational problems for shells of revolution. Others have suggested and used doubly curved elements (30) and curved frusta (31) for general shells of revolution. The recent application of the finite element method to the determination of the regions of dynamic instability of bars, plates, and complex structures for which other known techniques are unnecessarily difficult, has been the effort at Oklahoma State University (32) and (33). This thesis is an extension of these works to the dynamic stability of cylindrical shells under periodic axial and radial loading.

1.3 Finite Element Method

The finite element method consists basically of subdividing the structure into a number of elements, determining the behavioral characteristics of each element, and assembling the elements by connecting them at certain points or nodes in such a way so as to represent closely the original structure. The type of element to be used for a particular problem is very critical. The assembled elements must not only approximate the shape of the original structure, but must also be able to approximate the actions and deformations of the structure. If the properties of the material are known, then the behavior of each element can be described by relating the generalized forces to the generalized coordinates at the nodes. The behavior of the entire structure is then determined by satisfying compatibility of the elements at the nodes.

The finite element method is an approximate solution of a mathematical model of the real structure in contrast to other approximate methods which are approximate solutions of the governing differential equations of the problem. The governing differential equation is not necessary for the solution of a problem, and almost any boundary conditions can easily be applied. Many problems not readily handled by other means can be solved very efficiently by this method.

The matrices describing the response of an element can be derived by assuming either a displacement function throughout the element or a stress distribution within the element. However, since the effects of inertia and the potential energy due to loads are related directly to displacements and not stresses, a displacement function will be assumed for this study. A short cylinder, similar to the element that

Percy et al (27) used for the analysis of shells of revolution, will be assumed as a typical element.

1.4 Solution Procedure

The boundaries of the regions of dynamic instability are determined in the following steps:

a. Determine the equations of motion of a typical shell element.

b. Assume a displacement function for the shell element.

c. Derive the necessary influence matrices using stiffness formulation for the individual elements.

d. Assemble the elemental matrices to obtain the equation of motion of the entire shell.

e. Apply the boundary conditions.

f. Calculate the static buckling load and the natural frequency of the shell.

g. Determine the boundaries of the regions of dynamic instability by using the equations obtained in step d.

CHAPTER II

DERIVATION OF CONDITIONS OF INSTABILITY

2.1 Equation of Motion

The equations of motion of the system in finite element form are determined from a consideration of Hamilton's principle. The boundaries of the regions of dynamic instability are then derived from certain solutions of the equations of motion.

Hamilton's principle may be stated in the following manner (34):

$$\delta \int_{t_1}^{t_2} (T - W)\, dt = 0 \tag{1}$$

in which

T = kinetic energy,

W = the sum of the potential energy and the energy, dissipated by viscous damping,

t_1 = initial instant of time,

t_2 = final instant of time, and

δ indicates the first variation.

Equation (1) can be rewritten as:

$$\delta \int_{t_1}^{t_2} (T - U + V + \overline{W})\, dt = 0 \tag{2}$$

in which

U = strain energy

V = potential energy of the applied loads

$\overline{W}$ = energy dissipated by viscous damping.

The variation of equation (2) cannot be performed by the usual method due to the nonconservative energy, $\overline{W}$. However, equation (2) can be separated into two parts, conservative and nonconservative, as follows:

$$\delta \int_{t_1}^{t_2} (T - U + V)\, dt + \delta \int_{t_1}^{t_2} \overline{W}\, dt = 0. \tag{3}$$

The dissipated energy, $\overline{W}$, may be written as:

$$\overline{W} = \sum_i F_i \cdot d_i \tag{4}$$

in which

F_i = the ith damping force

d_i = the displacement at the point of application of the ith force.

Substituting equation (4) into the second integral in equation (3) yields:

$$\delta \int_{t_1}^{t_2} \overline{W}\, dt = \delta \int_{t_1}^{t_2} \sum_i F_i \cdot d_i\, dt. \tag{5}$$

Performing the variation on the right-hand side of equation (5) is equivalent to calculating the work done by the force F_i acting through a virtual displacement δd_i. Therefore, equation (5) may be rewritten in the following manner:

$$\delta \int_{t_1}^{t_2} \bar{W}\, dt = \int_{t_1}^{t_2} \sum_i F_i \cdot \delta d_i\, dt. \tag{6}$$

From the definition of generalized forces and generalized displacements the following expression can be written:

$$\sum_i F_i \cdot \delta d_i = \sum_j \bar{Q}_j \cdot \delta q_j \tag{7}$$

where $\bar{Q}_j$ is the jth generalized force due to damping forces and q_j is the jth generalized displacement. Substituting equation (7) into equation (5) and substituting the result into equation (3) yields:

$$\delta \int_{t_1}^{t_2} (T - U + V)\, dt + \int_{t_1}^{t_2} \sum_j \bar{Q}_j \cdot \delta q_j\, dt = 0. \tag{8}$$

The kinetic, strain, and potential energies can be defined in terms of the generalized velocities, $\{\dot{q}\}$, and the generalized displacements, $\{q\}$, as follows:

$$T = \frac{1}{2} (\dot{q})[m]\{\dot{q}\}$$

$$U = \frac{1}{2} (q)[k]\{q\}$$

$$V = \frac{p}{2} (q)[s]\{q\} + (Q)\{q\}$$

in which

[m] = mass matrix whose elements, m_{ij}, represent the ith inertia force due to the jth unit acceleration, all other accelerations being zero

[k] = stiffness matrix whose elements, k_{ij}, represent the ith external force due to the jth unit displacement, all other displacements being zero

[s] = stability matrix whose elements, s_{ij}, represent the out of plane component of the ith in plane load due to the jth unit displacement, all other displacements being zero.

p = the time dependent applied load.

Rayleigh's dissipation function may be written in matrix form as (35):

$$\mathring{W} = -\frac{1}{2}(\dot{q})[d]\{\dot{q}\} \tag{10}$$

in which

$\mathring{W}$ = one-half the time rate at which energy is dissipated by viscous damping, and

[d] = damping coefficient matrix whose elements, d_{ij}, represent the ith damping force due to the jth unit velocity, all other velocities being zero.

The damping force, $\overline{Q}_j$, is now given by:

$$\overline{Q}_j = \frac{\partial \mathring{W}}{\partial \dot{q}_j} \tag{11}$$

Performing the differentiation indicated in equation (11) on equation (10) gives:

$$\{\overline{Q}\} = -[d]\{\dot{q}\} . \tag{12}$$

Substituting equations (9) and (12) into equation (8) yields;

$$\delta \int_{t_1}^{t_2} \frac{1}{2}((\dot{q})[m]\{\ddot{q}\} - (q)[k]\{q\} + p(q)[s]\{q\} + (Q)\{\dot{q}\})\, dt - \int_{t_1}^{t_2} (\dot{q})[d]\, \delta\{q\}\, dt = 0. \tag{13}$$

By performing the variation of the first integral in equation (13) and combining the two integrals, Hamilton's equation becomes:

$$\int_{t_1}^{t_2} (-[m]\{\ddot{q}\} - [k]\{q\} + p[s]\{q\} + \{Q\} - [d]\{\dot{q}\})\,\delta\{q\}\,dt = 0 \quad (14)$$

The integral in equation (14) must be zero for any virtual displacement, $\delta\{q\}$; therefore, the term in parenthesis must vanish:

$$[m]\{\ddot{q}\} + [k]\{q\} - p[s]\{q\} + [d]\{\dot{q}\} = \{Q\}. \quad (15)$$

Equation (15) is the equation of motion of a typical element in terms of the mass, stiffness, stability, and damping coefficient matrices of that element. The equation of motion of the total structure is obtained by assembling the finite elements to form the complete structure. Performing this operation and denoting the assembled matrices by [K], [M], [S], and [D] yields:

$$[M]\{\ddot{q}\} + [K]\{q\} - p[S]\{q\} + [D]\{\dot{q}\} = 0 \quad (16)$$

which is the equation of motion of the entire structure.

2.2 Instability of Conservative Systems

If only conservative forces are considered i. e. the damping coefficient is zero, equation (16) becomes:

$$[M]\{\ddot{q}\} + [K]\{q\} - p[S]\{q\} = 0. \quad (17)$$

For the purpose of this study the time dependent load, p, will be assumed of the form:

$$p = p_o \pm p_t \cos \theta t \quad (18)$$

in which p_o is the constant portion of the load and p_t is the amplitude of the time dependent portion of the load. Substituting equation (18) into equation (17) leads to the equation of motion in the following form:

$$[M]\{\ddot{q}\} + [K]\{q\} - (p_o \pm p_t \cos \theta t)[S]\{q\} = 0. \qquad (19)$$

Three possibilities exist for parametrically excited lateral vibrations: 1. the vibrations may decrease in amplitude with time, 2. the vibrations may continue periodically, 3. the amplitudes of the vibrations may increase with time and eventually become unbounded. Bolotin (16) has shown that on the boundaries of the regions of instability the system of equations of the type of equation (19) has periodic solutions with a period of $T = \frac{2\pi}{\theta}$ or $2T = \frac{4\pi}{\theta}$. Also two solutions of identical periods bound the region of instability and two solutions of different periods bound the region of stability. From a physical observation it is seen that periodic solutions of the equations of motion form a boundary between regions in which vibrations decrease (regions of stability), and regions in which vibrations increase unboundedly (regions of instability).

The generalized displacements and accelerations in equation (19) are functions of time and position; however, to find a solution with a period of $2T = \frac{4\pi}{\theta}$ the generalized displacements are assumed in the form of an infinite series

$$\{q\} = \sum_{k=1,3,5..} \left\{ \{a_k\} \sin \frac{k\theta t}{2} + \{b_k\} \cos \frac{k\theta t}{2} \right\} \qquad (20)$$

in which $\{a_k\}$ and $\{b_k\}$ are independent of time. Substituting equation (20) into equation (19) and collecting similar terms of $\sin \frac{k\theta t}{2}$ and

$\cos \frac{k\theta t}{2}$ yields the following infinite number of matrix equations:

for $\sin \frac{k\theta t}{2}$

$$[[K] - p_o[S] + \frac{p_t}{2}[S] - \frac{\theta^2}{4}[M]]\{a_1\} - \frac{p_t}{2}[S]\{a_3\} = 0$$

$$[[K] - p_o[S] - \frac{k^2\theta^2}{4}[M]]\{a_k\} - \frac{p_t}{2}[S](\{a_{k-2}\} + \{a_{k+2}\}) = 0$$

$$(k=3,5,7\ldots) \qquad (21)$$

and for $\cos \frac{k\theta t}{2}$

$$[[K] - p_o[S] - \frac{p_t}{2}[S] - \frac{\theta^2}{4}[M]]\{b_1\} - \frac{p_t}{2}[S]\{b_3\} = 0$$

$$[[K] - p_o[S] - \frac{k^2\theta^2}{4}[M]]\{b_k\} - \frac{p_t}{2}[S](\{b_{k-2}\} + \{b_{k+2}\}) = 0$$

$$(k=3,5,7\ldots) \qquad (22)$$

The condition for a nontrivial solution of these equations is that the determinant of the coefficients of $\{a_k\}$ and $\{b_k\}$ must vanish. Combining the two determinants by using the $\pm$ sign yields:

$$\begin{vmatrix} [K]-(p_o \pm \frac{p_t}{2})[S]-\frac{\theta^2}{4}[M] & -\frac{1}{2}p_t[S] & 0 & \cdot \\ -\frac{1}{2}p_t[S] & [K]-p_o[S]-9\theta^2[M] & -\frac{1}{2}p_t[S] & \cdot \\ 0 & -\frac{1}{2}p_t[S] & [K]-p_o[S]-\frac{25\theta^2}{4}[M] & \cdot \\ \cdot & \cdot & \cdot & \cdot \\ \cdot & \cdot & \cdot & \cdot \end{vmatrix} = 0 \qquad (23)$$

If the series

$$\{q\} = \frac{1}{2}\{b_o\} + \sum_{k=2,4,6\ldots} \left[\{a_k\} \sin \frac{k\theta t}{2} + \{b_k\} \cos \frac{k\theta t}{2}\right] \qquad (24)$$

is substituted into equation (19), the following conditions for the existence of solutions with a period of $T = \frac{2\pi}{\theta}$ are found in a similar manner, giving:

$$\begin{vmatrix} [K]-p_o[S]-\theta^2[M] & -\frac{1}{2}p_t[S] & 0 & \cdot \\ -\frac{1}{2}p_t[S] & [K]-p_o[S]-4\theta^2[M] & -\frac{1}{2}p_t[S] & \cdot \\ 0 & -\frac{1}{2}p_t[S] & [K]-p_o[S]-16\theta^2[M] & \cdot \\ \cdot & \cdot & \cdot & \cdot \end{vmatrix} = 0 \qquad (25)$$

and

$$\begin{vmatrix} [K]-p_o[S] & -\frac{1}{2}p_t[S] & \cdot & \cdot \\ -\frac{1}{2}p_t[S] & [K]-p_o[S]-\theta^2[M] & -\frac{1}{2}p_t[S] & \cdot \\ 0 & -\frac{1}{2}p_t[S] & [K]-p_o[S]-4\theta^2[M] & \cdot \\ \cdot & \cdot & \cdot & \cdot \end{vmatrix} = 0 \qquad (26)$$

For an exact solution of the boundaries of the regions of instability, or if all of the regions of instability are desired, the infinite determinants of equations (23), (25), and (26) must be solved. However, only the principal regions which correspond to k = 1, are of practical importance in structural applications. A very good approximation to these regions can be obtained by considering only the first term on the principal diagonal of equation (23). This approximation

is equivalent to assuming that the generalized displacements, $\{q\}$, can be expressed with sufficient accuracy by considering only the first term of the infinite series of equation (20) as follows:

$$\{q\} = \{a_1\} \sin \frac{\theta t}{2} + \{b_1\} \cos \frac{\theta t}{2}. \tag{27}$$

Therefore, the solution of a dynamic stability problem for conservative systems reduces to finding the roots of the following determinant:

$$\left| [K] - (p_o \pm \frac{p_t}{2})[S] - \frac{\theta^2}{4}[M] \right| = 0 \tag{28}$$

2.3 Instability of Non-Conservative Systems

The equations of the boundaries of the principal regions of dynamic instability were derived in the previous section on the basis that all forces acting on the system are conservative. Therefore, no damping resistance is assumed to be present. Since it is known that most materials exhibit some damping characteristics, the effect of viscous damping on the boundaries of the regions of instability will be included in this section.

If equation (18) is substituted into equation (16) the equation of motion of the system becomes:

$$[M]\{\ddot{q}\} + [K]\{q\} - (p_o \pm p_t \cos \theta t)[S]\{q\} + [D]\{\dot{q}\} = 0 \tag{29}$$

Here again, the boundaries of the regions of instability are determined by finding periodic solutions with periods T of 2T for equation (28) in the same manner as for conservative problems. By substituting equation (20) into equation (29) solutions with a period of $2T = \frac{4\pi}{\theta}$

are found from the infinite number of matrix equations:

$$[[K] - p_o[S] - \frac{p_t}{2}[S] - \frac{\theta^2}{4}[M]]\{a_1\} - \theta[D]\{b_1\} - \frac{1}{2}p_t[S]\{a_3\} = 0$$

$$[[K] - p_o[S] - \frac{p_t}{2}[S] - \frac{\theta^2}{4}[M]]\{b_1\} + \theta[D]\{a_1\} - \frac{1}{2}p_t[S]\{b_3\} = 0$$

$$[[K] - p_o[S] - \frac{k^2\theta^2}{4}[M]]\{a_k\} - k\theta[D]\{b_k\}$$

$$- \frac{p_t}{2}[S]\{\{a_{k-2}\} + \{a_{k+2}\}\} = 0$$

$$[[K] - p_o[S] - k^2\theta^2[M]]\{b_k\} + k\theta[D]\{a_k\}$$

$$- \frac{p_t}{2}[S]\{\{b_{k-2}\} + \{b_{k+2}\}\} = 0 \qquad (30)$$

$$(k=3,5,7,\ldots)$$

For nontrivial solutions of equation (30) to exist the determinant of the coefficients of $\{a_k\}$ and $\{b_k\}$ must vanish. Therefore, the boundaries of the regions of instability including the effects of damping are located by solving the determinant given in Figure 1. As in the case of conservative problems, a good approximation to the boundaries of the principal regions can be obtained by considering only the first term of the infinite series in equation (20). Using this approximation the equations of the boundaries reduce to the requirement:

$$\begin{vmatrix} [K] - (p_o - \frac{p_t}{2})[S] - \frac{\theta^2}{4}[M] & -\theta[D] \\ \theta[D] & [K] - (p_o + \frac{p_t}{2})[S] - \frac{\theta^2}{4}[M] \end{vmatrix} = 0 \qquad (31)$$

$$\begin{bmatrix} \cdot & \cdot & \cdot & \cdot & \cdot \\ \cdot & [K]-p_o[S]-\frac{9\theta^2}{4}[M] & -\frac{p_t}{2}[S] & 0 & -3\theta[D] & \cdot \\ \cdot & -\frac{p_t}{2}[S] & [K]-(p_o-\frac{p_t}{2})[S]-\frac{\theta^2}{4}[M] & -\theta[D] & 0 & \cdot \\ \cdot & 0 & \theta[D] & [K]-(p_o+\frac{p_t}{2})[S]-\frac{\theta^2}{4}[M] & -\frac{p_t}{2}[S] & \cdot \\ \cdot & 3\theta[D] & 0 & -\frac{p_t}{2}[S] & [K]-p_o[S]-\frac{9\theta^2}{4}[M] & \cdot \\ \cdot & \cdot & \cdot & \cdot & \cdot & \cdot \end{bmatrix} = 0$$

Figure 1. Equations of the Boundaries of the Regions of Instability Including Damping

CHAPTER III

DERIVATION OF ELEMENTAL MATRICES

3.1 Displacement Function

An element with the assumed displacement coordinates and reference system is shown in Figure 2. The displacement coordinates, u, v, w, are the axial, tangential, and normal displacements, respectively. The individual elements are joined at the nodal circles. Accordingly, each element has four degrees of freedom at each end; three displacements and the rotation of a generator of the shell; a total of eight degrees of freedom. The assumed displacement function will have at least eight independent constants, one for each degree of freedom. If only eight constants were assumed the displacements would be:

$$\begin{aligned} u &= (A_1 + A_2 x) \cos n\phi \\ v &= (A_3 + A_4 x) \sin n\phi \\ w &= (A_5 + A_6 x + A_7 x^2 + A_8 x^3) \cos n\phi \end{aligned} \tag{32}$$

Pian (26) has developed a procedure to improve the accuracy of a stiffness matrix. More than the required number of constants are assumed in the displacement function, and the principle of minimum potential energy is utilized to evaluate the additional constants in terms of the generalized displacements of the element. This technique is used in this thesis, and is extended to improve the accuracy of the inertia and stability matrices.

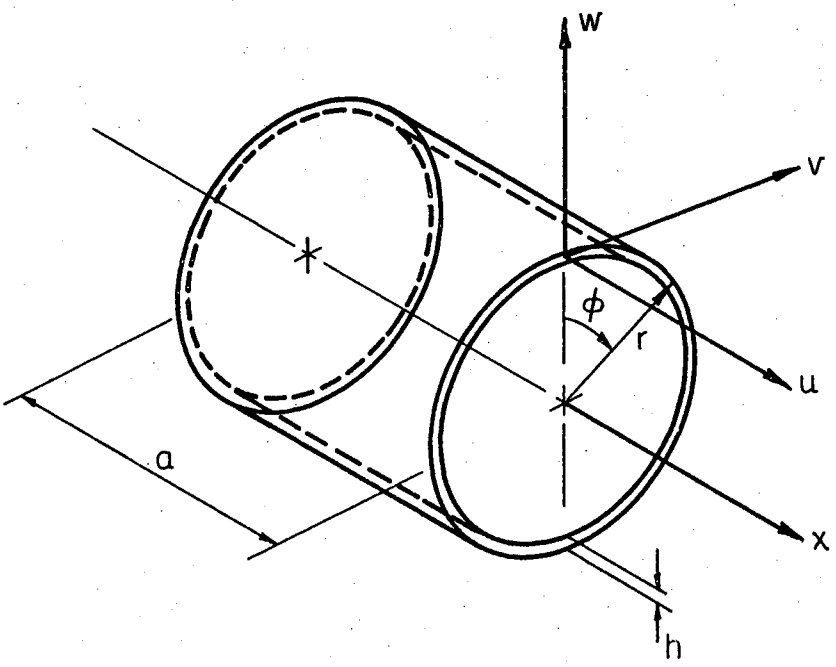

Figure 2. A Typical Shell Element

Four additional constants were chosen; therefore, the assumed displacement functions become:

$$u = (A_1 + A_2x + A_9x^2) \cos n\phi$$

$$v = (A_3 + A_4x + A_{10}x^2) \sin n\phi \tag{33}$$

$$w = (A_5 + A_6x + A_7x^2 + A_8x^3 + A_{11}x^4 + A_{12}x^5) \cos n\phi.$$

The rotation of a generator of the shell, γ, is then:

$$\gamma = \frac{\partial w}{\partial x}$$

or

$$\gamma = (A_6 + 2A_7x + 3A_8x^2 + 4A_{11}x^3 + 5A_{12}x^4) \cos n\phi. \tag{34}$$

3.2 Stiffness Matrix

a. Generalized displacements--The generalized displacements, q_i, are amplitudes of the assumed displacements at the ends of the element. By substituting the proper value of the x coordinate into the assumed displacements, the generalized coordinates can be written as:

$$\{q\} = [B_a \; B_b] \begin{Bmatrix} A_a \\ A_b \end{Bmatrix} \tag{35}$$

where $\{A_b\}$ is the column matrix of the four additional constants to the displacement function and the matrix $[B_a \; B_b]$ is listed in Figure 3.

Solving equation (35) for $\{A_a\}$ in terms of $\{q\}$, $[B_a]$, $[B_b]$ and $\{A_b\}$ gives:

$$\{A_a\} = [B_a^{-1} \vdots -B_a^{-1} B_b] \begin{Bmatrix} q \\ A_b \end{Bmatrix}. \tag{36}$$

$$\begin{bmatrix}
1 & 0 & 0 & 0 & 0 & 0 & 0 & 0 & 0 & 0 & 0 & 0 \\
0 & 0 & 1 & 0 & 0 & 0 & 0 & 0 & 0 & 0 & 0 & 0 \\
0 & 0 & 0 & 0 & 1 & 0 & 0 & 0 & 0 & 0 & 0 & 0 \\
0 & 0 & 0 & 0 & 0 & 1 & 0 & 0 & 0 & 0 & 0 & 0 \\
1 & a & 0 & 0 & 0 & 0 & 0 & 0 & a^2 & 0 & 0 & 0 \\
0 & 0 & 1 & a & 0 & 0 & 0 & 0 & 0 & a^2 & 0 & 0 \\
0 & 0 & 0 & 0 & 1 & a & a^2 & a^3 & 0 & 0 & a^4 & a^5 \\
0 & 0 & 0 & 0 & 0 & 1 & 2a & 3a^2 & 0 & 0 & 4a^3 & 5a^4
\end{bmatrix}$$

Figure 3. Matrix B_a B_b

Making use of the identity matrix, [I], the complete matrix of assumed constants, {A} can be expressed as:

$$\{A\} = [R] \begin{Bmatrix} q \\ A_b \end{Bmatrix} \tag{37}$$

where

$$[R] = \begin{bmatrix} B_a^{-1} & -B_a^{-1} B_b \\ 0 & I \end{bmatrix} \tag{38}$$

and

$$\{A\} = \begin{Bmatrix} A_a \\ A_b \end{Bmatrix}$$

Matrix [R] is listed in Figure 4. The solution of the dependent constants in terms of the generalized displacements is presented in section 3.2 e.

b. Strain-displacement relationships--The approximate equations relating the displacements in a thin cylindrical shell to the strains and curvature changes are (36):

$$\begin{aligned} \epsilon_x &= \frac{\partial u}{\partial x} \\ \epsilon_\phi &= \frac{1}{r}\frac{\partial v}{\partial \phi} + \frac{w}{r} \\ \epsilon_{x\phi} &= \frac{1}{r}\frac{\partial u}{\partial \phi} \quad \frac{\partial v}{\partial x} \\ k_x &= -\frac{\partial^2 w}{\partial x^2} \\ k_\phi &= -\frac{1}{r^2}\frac{\partial^2 w}{\partial \phi^2} + \frac{1}{r^2}\frac{\partial v}{\partial \phi} \\ k_{x\phi} &= -\frac{1}{r}\frac{\partial^2 w}{\partial x \partial \phi} + \frac{1}{r}\frac{\partial v}{\partial x}. \end{aligned} \tag{39}$$

$$
\begin{bmatrix}
1 & 0 & 0 & 0 & 0 & 0 & 0 & 0 & 0 & 0 & 0 & 0 \\
-\frac{1}{a} & 0 & 0 & 0 & \frac{1}{a} & 0 & 0 & 0 & -a & 0 & 0 & 0 \\
0 & 1 & 0 & 0 & 0 & 0 & 0 & 0 & 0 & 0 & 0 & 0 \\
0 & -\frac{1}{a} & 0 & 0 & 0 & \frac{1}{a} & 0 & 0 & 0 & -a & 0 & 0 \\
0 & 0 & 1 & 0 & 0 & 0 & 0 & 0 & 0 & 0 & 0 & 0 \\
0 & 0 & 0 & 1 & 0 & 0 & 0 & 0 & 0 & 0 & 0 & 0 \\
0 & 0 & -\frac{3}{a^2} & -\frac{2}{a} & 0 & 0 & \frac{3}{a^2} & -\frac{1}{a} & 0 & 0 & a^2 & 2a^3 \\
0 & 0 & \frac{2}{a^3} & \frac{1}{a^2} & 0 & 0 & -\frac{2}{a^3} & \frac{1}{a^2} & 0 & 0 & -2a & -3a^2 \\
0 & 0 & 0 & 0 & 0 & 0 & 0 & 0 & 1 & 0 & 0 & 0 \\
0 & 0 & 0 & 0 & 0 & 0 & 0 & 0 & 0 & 1 & 0 & 0 \\
0 & 0 & 0 & 0 & 0 & 0 & 0 & 0 & 0 & 0 & 1 & 0 \\
0 & 0 & 0 & 0 & 0 & 0 & 0 & 0 & 0 & 0 & 0 & 1
\end{bmatrix}
$$

Figure 4. Matrix [R]

Substituting the assumed displacement functions, equation (33), into equations (39), the strains can be related to the constants, $\{A\}$, by the equation:

$$\{\epsilon\} = [W]\{A\} \tag{40}$$

where the matrix [W] is given in Figure 5.

Utilizing equation (37) the strain matrix, equation (40) is expressed in terms of the generalized coordinates, $\{q\}$, and the dependent constants, $\{A_b\}$ as:

$$\{\epsilon\} = [W][R]\begin{Bmatrix} q \\ A_b \end{Bmatrix}. \tag{41}$$

c. Stress-resultants strain relationships--The relationship of the stress resultants to strains for a linearly elastic, isotropic, and homogeneous material may be written in matrix form as:

$$\{N\} = [H]\{\epsilon\}. \tag{42}$$

Equation (42) is written in expanded form in Figure 6.

d. Strain energy--The internal strain energy of an element can be expressed in matrix form in terms of stress-resultants and strains.

$$U = \frac{1}{2}\int_A \{\epsilon\}^T \{N\}\, dA \tag{43}$$

Using equation (42) which relates stress-resultants to the strains, the strain energy expression becomes:

$$U = \frac{1}{2}\int_A \{\epsilon\}^T [H]\{\epsilon\}\, dA. \tag{44}$$

Because the stress resultants and their corresponding strains were used

0	$\cos n\phi$	0	0	0	0	0	0	$2x \cos n\phi$	0	0	0
0	0	$\frac{n}{r} \cos n\phi$	$\frac{nx}{r} \cos n\phi$	$\frac{\cos}{r} n\phi$	$\frac{x}{r} \cos n\phi$	$\frac{x^2}{r} \cos n\phi$	$\frac{x^3}{r} \cos n\phi$	0	$\frac{nx^2}{r} \cos n\phi$	$\frac{x^4}{r} \cos n\phi$	$\frac{x^5}{r} \cos n\phi$
$-\frac{n}{r} \sin n\phi$	$-\frac{nx}{r} \sin n\phi$	0	$\sin n\phi$	0	0	0	0	$-\frac{nx^2}{r} \sin n\phi$	$2x \sin n\phi$	0	0
0	0	0	0	0	0	$-2 \cos n\phi$	$-6x \cos n\phi$	0	0	$-12x^2 \cos n\phi$	$-20x^3 \cos n\phi$
0	0	$\frac{n}{r^2} \cos n\phi$	$\frac{nx}{r^2} \cos n\phi$	$\frac{n^2}{r^2} \cos n\phi$	$\frac{n^2x}{r^2} \cos n\phi$	$\frac{n^2x^2}{r^2} \cos n\phi$	$\frac{n^2x^3}{r^2} \cos n\phi$	0	$\frac{nx^2}{r^2} \cos n\phi$	$\frac{n^2x^4}{r^2} \cos n\phi$	$\frac{n^2x^5}{r^2} \cos n\phi$
0	0	0	$\frac{\sin}{r} n\phi$	0	$\frac{n}{r} \sin n\phi$	$\frac{2nx}{r} \sin n\phi$	$\frac{3nx^2}{r} \sin n\phi$	0	$\frac{2x}{r} \sin n\phi$	$\frac{4nx^3}{r} \sin n\phi$	$\frac{5nx^4}{r} \sin n\phi$

Figure 5. Matrix [W]

$$\begin{bmatrix} N_x \\ N_\phi \\ N_{x\phi} \\ M_x \\ M_\phi \\ M_{x\phi} \end{bmatrix} = \begin{bmatrix} \frac{Eh}{1-\nu^2} & \frac{\nu Eh}{1-\nu^2} & 0 & 0 & 0 & 0 \\ \frac{\nu Eh}{1-\nu^2} & \frac{Eh}{1-\nu^2} & 0 & 0 & 0 & 0 \\ 0 & 0 & \frac{Eh}{2(1+\nu)} & 0 & 0 & 0 \\ 0 & 0 & 0 & \frac{Eh^3}{12(1-\nu^2)} & \frac{\nu Eh^3}{12(1-\nu^2)} & 0 \\ 0 & 0 & 0 & \frac{\nu Eh^3}{12(1-\nu^2)} & \frac{Eh^3}{12(1-\nu^2)} & 0 \\ 0 & 0 & 0 & 0 & 0 & \frac{Eh^3}{12(1+\nu)} \end{bmatrix} \begin{bmatrix} \epsilon_x \\ \epsilon_\phi \\ \epsilon_{x\phi} \\ K_x \\ K_\phi \\ K_{x\phi} \end{bmatrix}$$

Figure 6. Stress-Resultant Strain Relationships

in equation (42), equations (43) and (44) are integrated only over the surface of the element.

Substituting equation (41) into the strain energy expression, equation (44) yields:

$$U = \frac{1}{2}\int_A ((q,A_b)[R]^T[W]^T[H][W][R]\begin{Bmatrix} q \\ A_b \end{Bmatrix})\,dA. \tag{45}$$

The matrices (q,A_b) and $[R]$ are independent of the variables of integration in equation (45). Therefore,

$$U = \frac{1}{2}(q,A_b)[R]^T\left(\int_o^a \int_o^{2\pi} [W]^T[H][W]rd\phi dx\right)[R]\begin{Bmatrix} q \\ A_b \end{Bmatrix}. \tag{46}$$

Defining the matrix $[L]$ as:

$$[L] = \int_o^a \int_o^{2\pi} [W]^T[H][W]rd\phi dx \tag{47}$$

and performing the indicated matrix multiplication and integration, $[L]$, is evaluated and listed in Figure 7. Equation (46) now can be written as:

$$U = \frac{1}{2}(q,A_b)[R]^T[L]\begin{Bmatrix} q \\ A_b \end{Bmatrix} \tag{48}$$

or

$$U = \frac{1}{2}(q,A_b)\begin{bmatrix} K_{aa} & K_{ab} \\ K_{ba} & K_{bb} \end{bmatrix}\begin{Bmatrix} q \\ A_b \end{Bmatrix} \tag{49}$$

where

$$\begin{bmatrix} K_{aa} & K_{ab} \\ K_{ba} & K_{bb} \end{bmatrix} = [R]^T[L][R]. \tag{50}$$

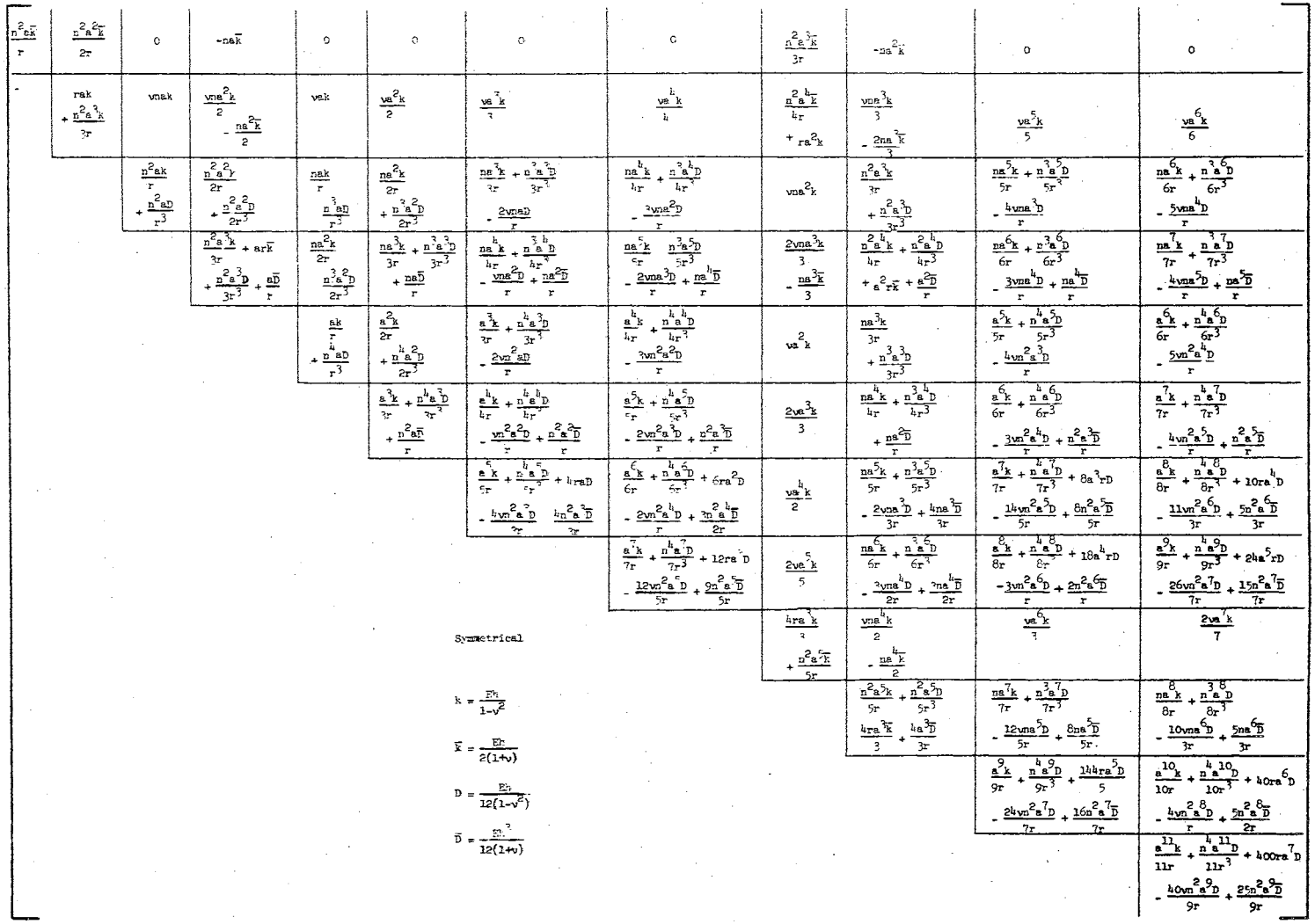

Symmetrical

$k = \frac{Eh}{1-\nu^2}$

$\bar{k} = \frac{Eh}{2(1+\nu)}$

$D = \frac{Eh^3}{12(1-\nu^2)}$

$\bar{D} = \frac{Eh^3}{12(1+\nu)}$

Figure 7. Matrix [L]

e. Total Potential Energy--The total potential energy including the work done by the generalized forces, $\{Q\}$, is:

$$\pi = U - (q)\{Q\} \tag{51}$$

which can be rewritten by using equation (49) as:

$$\pi = \frac{1}{2}(q,A_b)\begin{bmatrix} K_{aa} & K_{ab} \\ K_{ba} & K_{bb} \end{bmatrix}\begin{Bmatrix} q \\ A_b \end{Bmatrix} - (q)\{Q\}. \tag{52}$$

The theorem of minimum potential energy states that,"a conservative system is in a position of stable equilibrium if, and only if, the value of the potential energy is a relative minimum." Therefore, the partial derivative of the total potential energy with respect to the displacement coordinates is equal to zero, or for the case under consideration:

$$\begin{aligned} \frac{\partial \pi}{\partial q_i} &= 0 \qquad i = 1, 2 \ldots 8 \\ \frac{\partial \pi}{\partial A_i} &= 0 \qquad i = 9, \ldots 12. \end{aligned} \tag{53}$$

Performing the indicated partial differentiation on equation (52) yields:

$$\begin{bmatrix} K_{aa} & K_{ab} \\ K_{ba} & K_{bb} \end{bmatrix}\begin{Bmatrix} q \\ A_b \end{Bmatrix} = \begin{Bmatrix} Q \\ \cdots \\ 0 \end{Bmatrix}. \tag{54}$$

Solving the last four equations of this relation for the dependent constants, $\{A_b\}$ in terms of the generalized coordinates, $\{q\}$, gives:

$$\{A_b\} = - [K_{bb}]^{-1}[K_{ba}]\{q\}. \tag{55}$$

The first eight equations of equation (54) can be written as:

$$[K_{aa}]\{q\} + [K_{ab}]\{A_b\} = \{Q\}. \tag{56}$$

Substituting equation (55) into equation (56) gives the following:

$$[[K_{aa}] - [K_{ab}][K_{bb}]^{-1}[K_{ba}]]\{q\} = \{Q\}. \tag{57}$$

Then by definition, the element stiffness matrix, [k], is:

$$[k] = [K_{aa}] - [K_{ab}][K_{bb}]^{-1}[K_{ba}]. \tag{58}$$

3.3 Mass Matrix

The inertia forces developed at the nodal circles on each end of an element are derived by considering the total kinetic energy of the element. A velocity distribution over the surface of the element, similar to the displacement function used in deriving the stiffness matrix, is assumed as the following:

$$\begin{aligned} \dot{u} &= (\dot{A}_1 + \dot{A}_2 x + \dot{A}_9 x^2) \cos n\phi \\ \dot{v} &= (\dot{A}_3 + \dot{A}_4 x + \dot{A}_{10} x^2) \sin n\phi \\ \dot{w} &= (\dot{A}_5 + \dot{A}_6 x + \dot{A}_7 x^2 + \dot{A}_8 x^3 + \dot{A}_{11} x^4 + \dot{A}_{12} x^5) \cos n\phi. \end{aligned} \tag{59}$$

The total kinetic energy, T, of an element is:

$$T = \frac{\rho h}{2} \int_A (\dot{u}^2 + \dot{v}^2 + \dot{w}^2)\, dA \tag{60}$$

or by including the proper limits of integration,

$$T = \frac{\rho h}{2} \int_0^a \int_0^{2\pi} (\dot{u}^2 + \dot{v}^2 + \dot{w}^2)\, r\, d\phi\, dx \tag{61}$$

where ρ is the mass density of the material per unit volume. Substituting the assumed velocity distribution into the kinetic energy expression, equation (61), and performing the integration yields:

$$T = \frac{\rho h \pi r}{2} \{\dot{A}\}^T [V] \{\dot{A}\} \tag{62}$$

where matrix [V] is listed in Figure 8.

In the previous section a relation was developed between the constants of the assumed displacement function, $\{A\}$, and the generalized displacements $\{q\}$. This relation depends only on the form of the displacement function and the geometric properties of the element. The velocity distribution, assumed in this section, has exactly the same form as the displacement function of the preceding section. Therefore, the assumed velocity constants, $\{\dot{A}\}$ are related to the generalized velocities, $\{\dot{q}\}$, by the same matrix as the displacement constants are to the generalized displacements. From equation (36) the following equation is obtained

$$\{\dot{A}\} = \begin{bmatrix} B_a^{-1} & -B_a^{-1} B_b \\ 0 & I \end{bmatrix} \begin{Bmatrix} \dot{q} \\ A_b \end{Bmatrix} \tag{63}$$

and from equation (55)

$$\{\dot{A}_b\} = -[K_{bb}]^{-1} [K_{ba}] \{\dot{q}\}. \tag{64}$$

Using equation (64) and the identity matrix, [I], the following expression can be written:

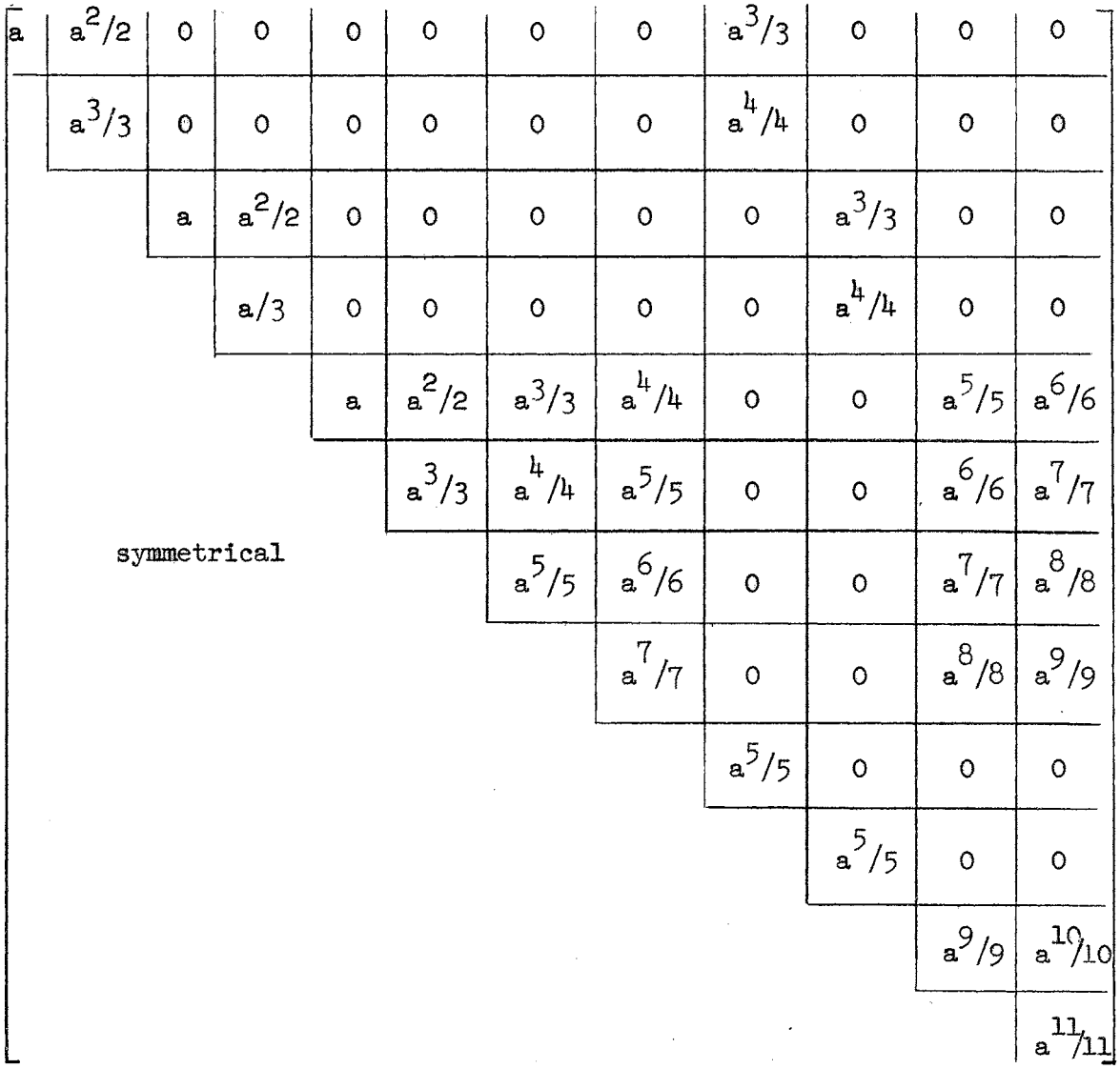

Figure 8. Matrix [V]

$$\begin{Bmatrix} \dot{q} \\ \dot{A}_b \end{Bmatrix} = \begin{bmatrix} I & 0 \\ -[K_{bb}]^{-1} & [K_{ba}] \end{bmatrix} \{\dot{q}\}. \tag{65}$$

The complete matrix of velocity constants can now be written in terms of the generalized velocities by substituting equation (65) into equation (63) which yields:

$$\{\dot{A}\} = \begin{bmatrix} B_a^{-1} & -B_a^{-1}B_b \\ 0 & I \end{bmatrix} \begin{bmatrix} I & \\ -K_{bb} & {}^{-1}K_{ba} \end{bmatrix} \{\dot{q}\} \tag{66}$$

or

$$\{\dot{A}\} = [\bar{R}]\{\dot{q}\} \tag{67}$$

where

$$[\bar{R}] = \begin{bmatrix} B_a^{-1} & -B_a^{-1}B_b \\ 0 & I \end{bmatrix} \begin{bmatrix} I & \\ -K_{bb} & {}^{-1}K_{ba} \end{bmatrix}. \tag{68}$$

The kinetic energy of the element can now be written in terms of the generalized velocities by substituting equation (67) into equation (62) giving:

$$T = \frac{\rho h \pi r}{2} (\dot{q})[\bar{R}]^T[V][\bar{R}]\{\dot{q}\}. \tag{69}$$

It follows directly from equation (9) that the mass matrix [m] is:

$$[m] = \rho h \pi r\, [\bar{R}]^T[V][\bar{R}]. \tag{70}$$

3.4 Stability Matrix

The work done by the parametric loads acting through the bending

displacements of a shell element is used as a basis to derive the stability matrix. The axial bending deformation of a cylindrical element subjected to an axial load is:

$$\Delta L = \frac{1}{2}\int_o^a \left(\left(\frac{\partial v}{\partial x}\right)^2 + \left(\frac{\partial w}{\partial x}\right)^2\right) dx, \tag{71}$$

and the work done by a uniform axial load is:

$$W_A = \int_o^{2\pi} N_x \Delta L \, r d\phi \tag{72}$$

or

$$W_A = \frac{N_x}{2}\int_o^{2\pi}\int_o^a \left(\left(\frac{\partial v}{\partial x}\right)^2 + \left(\frac{\partial w}{\partial x}\right)^2\right) r dx d\phi. \tag{73}$$

The shortening of the mean circumference of a cylindrical element due to bending displacements is:

$$\Delta C = \frac{1}{2}\int_o^{2\pi} \frac{1}{r^2}\left(\frac{\partial w}{\partial \phi}\right)^2 r d\phi \tag{74}$$

and the work done by a uniform radial pressure becomes:

$$W_\phi = \frac{N\phi}{2}\int_o^a \int_o^{2\pi} \frac{1}{r}\left(\frac{\partial w}{\partial \phi}\right)^2 d\phi dx. \tag{75}$$

By combining equations (73) and (75) the total work done by the external loads is:

$$W_T = \frac{1}{2}\int_o^a \int_o^{2\pi}\left(\frac{N\phi}{r^2}\left(\frac{\partial w}{\partial \phi}\right)^2 + N_x\left(\frac{\partial v}{\partial x}\right)^2 + \left(\frac{\partial w}{\partial x}\right)^2\right) r d\phi dx. \tag{76}$$

Substituting the assumed displacement function into equation (76) and performing the integration yields:

$$W_T = \frac{p}{2} (A) [P] \{A\} \tag{77}$$

and by substituting equation (67) into this relation,

$$W_T = \frac{p}{2} (q) [\bar{R}]^T [P] [\bar{R}] \{q\} \tag{78}$$

where matrix [P] is listed in Figure 9. The stability matrix, [s], is now:

$$p[s] = \frac{\partial^2 W_T}{\partial q^2} \tag{79}$$

or

$$[s] = [\bar{R}]^T [P] [\bar{R}]. \tag{80}$$

3.5 Damping Matrix

The damping forces developed at the nodal circles are derived from the time rate at which energy is dissipated by viscous damping. The damping forces in the shell are assumed to be directly proportional to the velocity. Therefore, one-half the rate at which energy is dissipated is:

$$\dot{W} = \frac{1}{2} c \int_o^a \int_o^{2\pi} (\dot{u}^2 + \dot{v}^2 + \dot{w}^2) \, r d\phi dx \tag{81}$$

where c is the damping coefficient of the material. Comparing this relation with equation (61) it follows that:

$$\dot{W} = \frac{c}{\rho h} T. \tag{82}$$

Therefore, the damping matrix, [d] is the following:

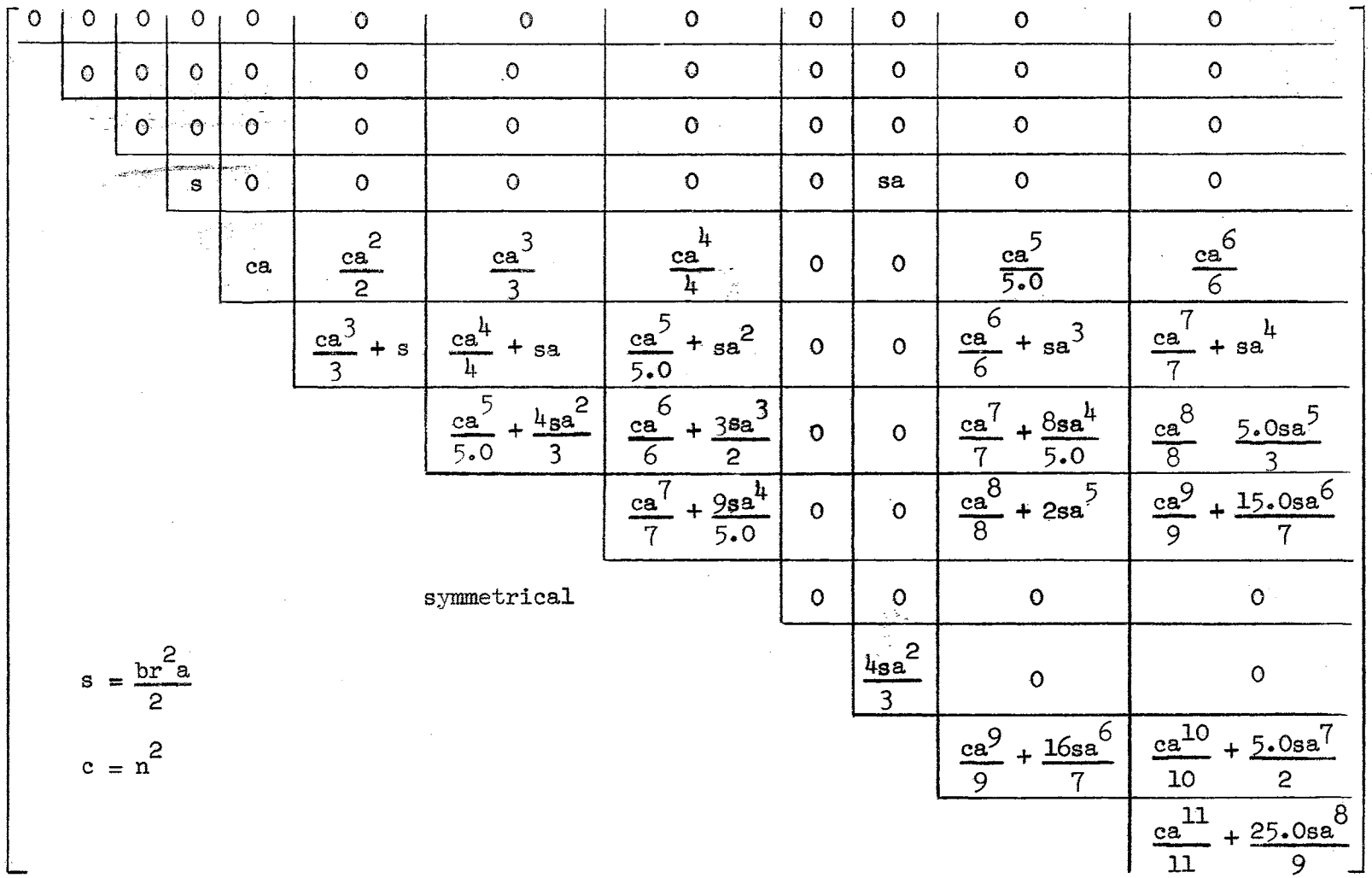

Figure 9. Matrix [P]

$$[d] = \frac{c}{\rho h}\,[m]. \tag{83}$$

3.6 Alternate Displacement Function

The stiffness, mass, stability, and damping matrices for an element were derived in the preceding sections of this chapter on the basis of an assumed displacement field with twelve terms, as in equation (33). Another displacement function with more terms was also used as follows:

$$\begin{aligned} u &= (A_1 + A_2 x + A_9 x^2 + A_{13} x^3) \cos n\phi \\ v &= (A_3 + A_4 x + A_{10} x^2 + A_{14} x^3) \sin n\phi \\ w &= (A_5 + A_6 x + A_7 x^2 + A_8 x^3 + A_{11} x^4 + A_{12} x^5) \cos n\phi. \end{aligned} \tag{84}$$

The procedure for calculating the elemental matrices using equation (84) for the assumed displacement field is identical to the procedure when equation (33) was assumed for the displacements. However, the order of the matrices [L], [R], [V], and [P] is fourteen for this case instead of twelve. The first twelve rows and columns would be the same for both cases. The thirteenth and fourteenth columns of the symmetrical matrices [R], [L], [V], and [P] are listed in Figures 10, 11, 12, and 13 respectively.

$$\begin{bmatrix} 0 & 0 \\ -a^2 & 0 \\ 0 & 0 \\ 0 & -a^2 \\ 0 & 0 \\ 0 & 0 \\ 0 & 0 \\ 0 & 0 \\ 0 & 0 \\ 0 & 0 \\ 0 & 0 \\ 0 & 0 \\ 1 & 0 \\ 0 & 1 \end{bmatrix}$$

Figure 10. Columns Thirteen and Fourteen of Matrix [R]

$\frac{n^2a^4\overline{k}}{4r}$	$-na^3\overline{k}$
$\frac{n^2a^5\overline{k}}{5r} + a^3rk$	$-\frac{3na^4\overline{k}}{4} + \frac{\nu na^4k}{4}$
νna^3k	$\frac{n^2a^4k}{4r} + \frac{n^2a^4D}{4r^3}$
$\frac{3\nu na^4k}{4} - \frac{na^4\overline{k}}{4}$	$\frac{n^2a^5k}{5r} + \frac{n^2a^5D}{5r^3} + ra^3\overline{k} + \frac{a^3\overline{D}}{r}$
νa^3k	$\frac{na^4k}{4r} + \frac{n^3a^4D}{4r^3}$
$\frac{3\nu a^4k}{4}$	$\frac{na^5k}{5r} + \frac{n^3a^5D}{5r^3} + \frac{na^3\overline{D}}{r}$
$\frac{3\nu a^5k}{5}$	$\frac{na^6k}{6r} + \frac{n^3a^6D}{6r^3} - \frac{\nu na^4D}{2r} + \frac{3na^4\overline{D}}{2r}$
$\frac{\nu a^6k}{2}$	$\frac{na^7k}{7r} + \frac{n^3a^7D}{7r^3} - \frac{6\nu na^5D}{5r} + \frac{9na^5\overline{D}}{5r}$
$\frac{3ra^4k}{2} + \frac{n^2a^6\overline{k}}{6r}$	$\frac{2\nu a^5nk}{5} - \frac{3na^5\overline{k}}{5}$
$\frac{3\nu na^5k}{5} - \frac{2na^5\overline{k}}{5}$	$\frac{n^2a^6k}{6r} + \frac{n^2a^6D}{6r^3} + \frac{3ra^4\overline{k}}{2} + \frac{3a^4\overline{D}}{2r}$
$\frac{3\nu a^7k}{7}$	$\frac{na^8k}{8r} + \frac{n^3a^8D}{8r^3} - \frac{2\nu na^6D}{r} + \frac{2na^6\overline{D}}{r}$
$\frac{3\nu a^8k}{8}$	$\frac{na^9k}{9r} + \frac{n^3a^9D}{9r^3} - \frac{20\nu na^7D}{7r} + \frac{15na^7\overline{D}}{7r}$
$\frac{9ra^5k}{5} + \frac{n^2a^7\overline{k}}{7r}$	$\frac{\nu na^6k}{2} - \frac{na^6\overline{k}}{2}$
$\frac{\nu na^6k}{2} - \frac{na^6\overline{k}}{2}$	$\frac{n^2a^7k}{7r} + \frac{n^2a^7D}{7r^3} + \frac{9ra^5\overline{k}}{5} + \frac{9a^5\overline{D}}{5r}$

Figure 11. Columns Thirteen and Fourteen of Matrix [L]

$$\begin{bmatrix} a^4/4 & 0 \\ a^5/5 & 0 \\ 0 & a^4/4 \\ 0 & a^5/5 \\ 0 & 0 \\ 0 & 0 \\ 0 & 0 \\ 0 & 0 \\ a^6/6 & 0 \\ 0 & a^6/6 \\ 0 & 0 \\ 0 & 0 \\ a^7/7 & 0 \\ 0 & a^7/7 \end{bmatrix}$$

Figure 12. Columns Thirteen and Fourteen of Matrix [V]

$$\begin{bmatrix} 0 & 0 \\ 0 & 0 \\ 0 & 0 \\ 0 & sa^2 \\ 0 & 0 \\ 0 & 0 \\ 0 & 0 \\ 0 & 0 \\ 0 & 0 \\ 0 & 3sa^3/2 \\ 0 & 0 \\ 0 & 0 \\ 0 & 0 \\ 0 & 9sa^4/5.0 \end{bmatrix}$$

Figure 13. Columns Thirteen and Fourteen of Matrix [P]

CHAPTER IV

FORMULATION OF THE SOLUTION

In Chapter II the equations for determining the boundaries of the principal regions of dynamic instability were derived in terms of the stiffness, mass, stability, and damping coefficient matrices of some arbitrary structure. In this analysis the type of the structure and its deformations remained general. The stiffness, mass, stability, and damping coefficient matrices for a right circular cylindrical shell element were derived in Chapter III. These matrices were derived by assuming that the deformation of the shell could be expressed as the product of a polynomial function of the axial coordinate and a cosine function of the central angle. The node circles along the axis of the shell allows an arbitrary deformation along the axis of the shell but restricts the deformation around the circumference to a predetermined number of cosine waves. The number of cosine waves, n, is treated as a parameter so that any number of waves around the circumference of the shell can be investigated. It is the purpose of this chapter to formulate the equations needed to solve the problem being considered in final form. The general problem which is solved in this thesis is shown in Figure 14.

4.1 Formation of the Structural Matrices

The shell being analyzed is first divided into a number of finite

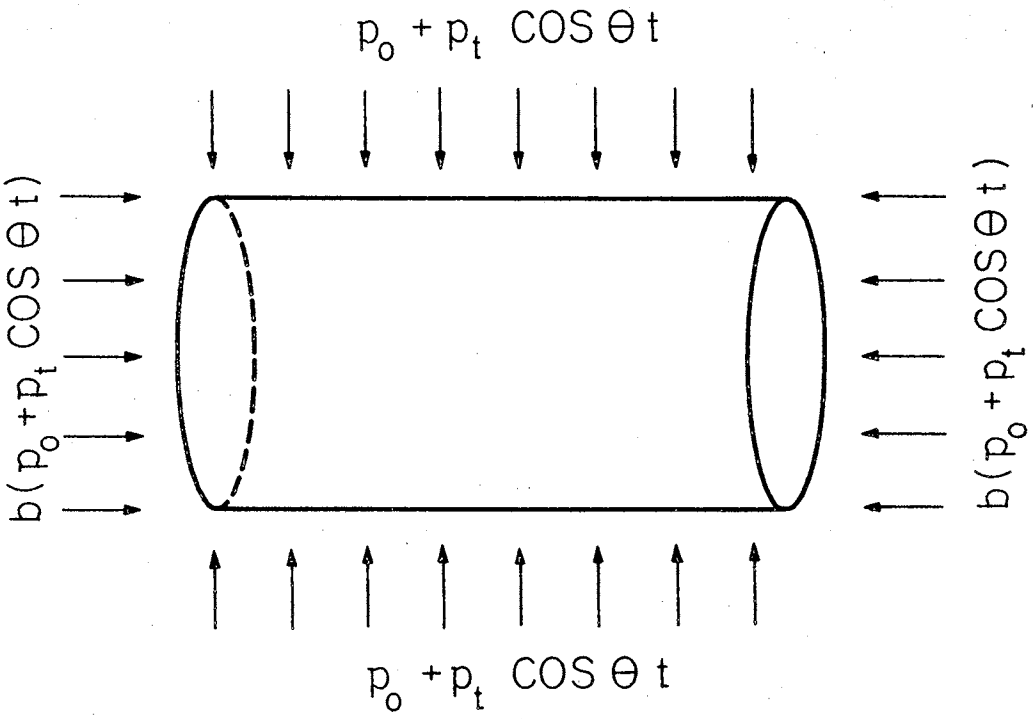

Figure 14. Shell with General Loading

elements. The stiffness properties of each element are calculated by the equations developed in Chapter III. The total structural matrices are formed from the elemental matrices by establishing compatibility at the nodal circles (the ends of each finite element) which is accomplished by adding corresponding coefficients at each node circle. After the total structural matrices are formed the support conditions of the shell must be applied. This is easily accomplished by deleting the row and column in the total structural matrix which corresponds to each boundary constraint. The term structural matrix will be used hereafter to apply to the total structural matrix after the boundary conditions have been applied.

The order of the elemental matrix for the cylindrical element is eight and the order of the structural matrix is $(4j + 4-b)$, where j is the number of finite elements into which the shell is divided and b is the number of boundary constraints. The choice of the number of elements is often a compromise between accuracy and computing time. The number of nodes must be sufficient to represent accurately the deformation of the shell but, if too many elements are chosen, the computation time becomes excessive.

4.2 Equations of the Solution

The equation of motion of a shell without damping is given by equation (19) as:

$$[M]\{\ddot{q}\} + [K]\{q\} - (p_o \pm p_t \cos \theta t)[S]\{q\} = 0. \qquad (85)$$

For the case of static buckling $\{\ddot{q}\}$ and p_t are zero; therefore, equation (85) reduces to the following:

$$[[K] - p_o[S]]\{q\} = 0. \tag{86}$$

The static buckling loads are the values of p_o which make the determinant of the coefficients of $\{q\}$ vanish or:

$$\left|[K] - p_o[S]\right| = 0. \tag{87}$$

If the shell is vibrating freely then p_o and p_t vanish and equation (85) becomes:

$$[M]\{\ddot{q}\} + [K]\{q\} = 0. \tag{88}$$

For harmonic vibrations the generalized displacements, $\{q\}$, may be represented in the following form:

$$\{q\} = \{\bar{q}\}\sin\omega t \tag{89}$$

where $\{\bar{q}\}$ is independent of time. Substituting equation (89) into equation (88) yields:

$$[[K] - \omega^2 [M]]\{\bar{q}\}\sin\omega t = 0. \tag{90}$$

The condition for nontrivial solutions of equation (90) requires that the determinant of the coefficients of $\{\bar{q}\}$ must vanish. Therefore, the natural frequencies of a cylindrical shell are given by the following equation:

$$\left|[K] - \omega^2 [M]\right| = 0. \tag{91}$$

For a shell vibrating under the action of a constant load equation (85) reduces to:

$$[M]\{\ddot{q}\} + [K]\{q\} - p_o[S]\{q\} = 0. \tag{92}$$

Substituting equation (89) into equation (92) the frequencies of free vibration of a shell under a constant load are given by:

$$\left|[K] - p_o[S] - \omega^2 [M]\right| = 0. \tag{93}$$

For the problem of dynamic stability, the constant and pulsating portions of the load, p_o and p_t, may be defined by:

$$\begin{aligned} p_o &= \alpha p^* \\ p_t &= \beta p^* \end{aligned} \tag{94}$$

where p^* is the lowest buckling load as determined from equation (87). Substituting equation (94) into equation (28) the boundaries of the principal regions of dynamic instability excluding damping are located by the following relation:

$$\left|[K] - (\alpha \pm \frac{\beta}{2})\, p^*[S] - \frac{\theta^2}{4}[M]\right| = 0. \tag{95}$$

Similarly the determinant for determining the principal regions of instability with viscous damping is found by substituting equation (94) into equation (31) which yields:

$$\begin{vmatrix} [K] - (\alpha + \frac{\beta}{2})p^*[S] - \frac{\theta^2}{4}[M] & -\frac{c\theta}{\rho h}[M] \\ \frac{c\theta}{\rho h}[M] & [K] - (\alpha - \frac{\beta}{2})p^*[S] - \frac{\theta^2}{4}[M] \end{vmatrix} = 0 \tag{96}$$

CHAPTER V

PRESENTATION OF RESULTS

The static buckling loads, natural frequencies, and boundaries of the regions of dynamic instability without damping for a cylindrical shell are found by calculating the eigenvalues of equations (87), (91), and (95). The eigenvectors associated with the eigenvalues represent the characteristic shapes (mode shapes) of the deformed structure. The boundaries of the regions of instability including viscous damping are determined by finding the values of the frequency, θ, which cause the determinant in equation (96) to be zero for arbitrary values of the applied load. A trial and error procedure is necessary to do this because the form of this equation will not allow a direct solution. Points within the regions of instability indicate a dynamically unstable shell for the corresponding parameters. A program was written for the IBM 7040 electronic digital computer to formulate the stiffness, mass, and stability matrices from given shell dimensions and boundary conditions and to calculate the desired values from equations (87), (91), (95), and (96).

5.1 Free Vibration

The natural frequencies of a cylindrical shell are found by solving equation (91). Two examples were solved for comparison with existing solutions: an analytical solution of a cylinder clamped on both

ends (37) and some experimental results for a simply supported cylinder (38). The results of these examples are shown in Table I. and Table II. The effect of the number of constants in the assumed displacement function on the accuracy of the calculated natural frequencies is shown in Table I. At first only the eight independent constants were used, but the results were not in close agreement with existing solutions. Twelve terms were assumed in the displacement function: three terms for u, three terms for v, and six terms for w as follows:

$$\begin{aligned} u &= (A_1 + A_2 x + A_9 x^2) \cos n\phi \\ v &= (A_3 + A_4 x + A_{10} x^2) \sin n\phi \\ w &= (A_5 + A_6 x + A_7 x^2 + A_8 x^3 + A_{11} x^4 + A_{12} x^5) \cos n\phi. \end{aligned} \tag{97}$$

Also, fourteen terms were assumed in another attempt to improve the displacement function. These were taken as follows:

$$\begin{aligned} u &= (A_1 + A_2 x + A_9 x^2 + A_{13} x^3) \cos n\phi \\ v &= (A_3 + A_4 x + A_{10} x^2 + A_{14} x^3) \sin n\phi \\ w &= (A_5 + A_6 x + A_7 x^2 + A_8 x^3 + A_{11} x^4 + A_{12} x^5) \cos n\phi. \end{aligned} \tag{98}$$

As is seen from Table I, better results were obtained from the 12-term displacement field than for 8-terms. Still, better overall results were obtained from the 14-term field when compared with that for 12-terms. This was found to be the case especially for higher mode shapes along the axis of the shell (larger values of m).

TABLE I

NATURAL FREQUENCIES OF A CYLINDER
CLAMPED ON BOTH ENDS

$E = 30 \times 10^6$ lb/in^2 $\quad$ h = 0.1 inch

Density = 0.283 lb/in^3 $\quad$ r = 3.0 inches

$\nu = 0.3$ $\quad$ L = 12.0 inches

	m = 1				m = 3			
n	8 A's	12 A's	14 A's	Kraus	8 A's	12 A's	14 A's	Kraus
3	1295	1180	1178	1176	4750	4520	4365	4350
4	919	782	776	783	3650	3210	3103	3139
5	737	589	585	597	2950	2400	2304	2342
6	680	541	537	552	2480	1890	1793	1823
7	711	598	596	611	2170	1570	1479	1503
8	812	725	725	736	1990	1400	1321	1338
9	957	884	900	902	1900	1360	1293	1302
10	1140	1110	1112	1100	1890	1430	1373	1369
11	1350	1360	1362	1321	1955	1590	1538	1512

TABLE II

NATURAL FREQUENCIES OF A SIMPLY SUPPORTED CYLINDER

$E = 29.6 \times 10^6$ lb/in^2 $\quad$ h = 0.101 inch

Density = 0.283 lb/in^3 $\quad$ r = 1.924 inches

$\nu = 0.29$ $\quad$ L = 15.63 inches

	m = 1		m = 2		m = 3		m = 4	
n	Finite Element	Exp.*	Finite Element	Exp.*	Finite Element	Exp.*	Finite Element	Exp.*
2	898	960	2080	2070	3900	3725	5960	5270
3	2150	2130	2320	2420	3140	3130	4190	4180
4	3960	3985	4075	4130	4360	4430	4890	4950
5	6620	6400	6700	6500	6880	6700	7210	7030
6	10100	9270	10200	9370	10350	9570	10600	9850

* Arnold and Warburton (38)

A solution was attempted using sixteen terms in the displacement function which consisted of adding two more terms to the expression for w in equation (98) but for this case the stiffness matrix became improper. No further attempt was made to refine the displacement function more than the fourteen terms used in this section.

5.2 Static Buckling

The static buckling loads and their associated characteristic shapes are found by solving equation (87). The buckling problem is divided into three categories for this study; radial pressure only, axial pressure only, and combined axial and radial pressure. Each of these cases is compared with an analytical solution for a simply supported cylinder (39). The cylinder used throughout the rest of this study has the following dimensions and properties:

$$L = 25.0 \text{ inches}$$

$$r = 2.0 \text{ inches}$$

$$h = 0.01 \text{ inch}$$

$$\nu = 0.25 \ .$$

Table III gives the critical external radial pressure for several mode shapes. It is noted that for the primary mode shape along the axis of the cylinder the displacement function with only eight constants gives values closer to the analytical solution than the finite element solution involving a more refined displacement function. However, the solution with eight constants requires a larger number of elements than the refined displacement field as shown in Table IV, and the convergence is not uniform. In addition to this, the solutions

TABLE III

BUCKLING PRESSURES FOR A SIMPLY SUPPORTED CYLINDER SUBJECTED TO A UNIFORM RADIAL LOAD

$p^* = \bar{p}E \times 10^{-7}$ lb/in^2

	m = 1				m = 2			
n	8 A's	12 A's	14 A's	Flugge	8 A's	12 A's	14 A's	Flugge
2	4.22	3.28	3.28	4.43	58.4	44.5	44.7	60.3
3	1.33	1.07	1.07	1.22	8.33	4.97	4.97	5.63
4	1.75	1.62	1.62	1.74	3.69	2.35	2.35	2.54
5	2.67	2.60	2.60	2.70	3.50	2.80	2.81	2.94
6	3.86	3.86	3.87	3.91	4.33	3.91	3.96	4.02
7	5.29	5.44	5.46	5.35	5.60	5.37	5.51	5.42

TABLE IV

BUCKLING PRESSURES OF A CYLINDER UNDER RAIDAL LOAD
FOR DIFFERENT NUMBER OF FINITE ELEMENTS

$p^* = \bar{p}E \times 10^{-7}$ psi

	8 term displacement field					14 term displacement field		
n	5 Elements	8 Elements	10 Elements	16 Elements	20 Elements	5 Elements	10 Elements	Flugge
2			4.22	3.40		3.28	3.28	4.43
3	2.62	1.50	1.33	1.22	1.29	1.08	1.07	1.22
4	2.35	1.82	1.75	1.75	1.81	1.63	1.62	1.74
5	2.99	2.70	2.67			2.61	2.60	2.70
6			3.86				3.87	3.91
7			5.29				5.46	5.35

with more terms in the displacement function yield much better accuracy for higher modes along the axis of the cylinder.

The critical stresses for the assumed cylinder subjected to uniform axial pressure are given in Table V for a few mode shapes. In this case the results obtained by using only eight constants in the displacement function do not even approximate the analytical results. An attempt was made to overcome this deficiency by using a larger number of finite elements, but this helped very little. It was this problem which made a refinement of the assumed displacement function necessary. Assuming a displacement function with twelve constants yields results which compare favorably with the analytical solution for most of the mode shapes given. However, increasing the number of constants to fourteen gave even a better comparison, especially for higher modes along the axis of the cylinder. Also, the displacement fields with eight and twelve terms often gave critical mode shapes which differed from those predicted by the analytical solution. These are marked by * to the left.

Table VI gives the buckling loads for combined loading for one ratio of end pressure to radial pressure and for three different boundary conditions. It was necessary for the ratio of end pressure to radial pressure to be large, for the assumed shell dimensions, to obtain a solution that differed from the case of radial pressure only.

On the basis of the comparisons made in sections 5.1 and 5.2 it was concluded that the displacement function containing fourteen terms should give better results in the remaining analysis.

TABLE V

CRITICAL STRESSES IN A SIMPLY SUPPORTED CYLINDER
UNDER AN AXIAL LOAD

$\sigma^* = \bar{p}E \times 10^{-4}$ psi

	1st Critical Stress					2nd Critical Stress				
n	m	8 A's	12 A's	14 A's	Flugge	m	8 A's	12 A's	14 A's	Flugge
2	1	42.3	33.2	33.2	34.3	2	147	112	112	115
3	1	34.0	27.4	27.3	27.5	2	53.1	31.9	31.8	32.1
4	2	43.7	28.1	28.1	28.2	3	59.7	28.5	28.3	28.5
5	3 4	*55.4	27.9	27.5	27.6	2 5 3	*66.0	31.0	30.5	30.4
6	4 6	*66.4	30.2	28.5	28.3	3 5	*72.0	29.9	29.2	29.2
7	5 8	*76.0	33.7	29.0	28.7	4 9 7	*81.4	*32.3	29.4	29.2

TABLE VI

BUCKLING PRESSURES FOR A CYLINDER
UNDER COMBINED LOADING

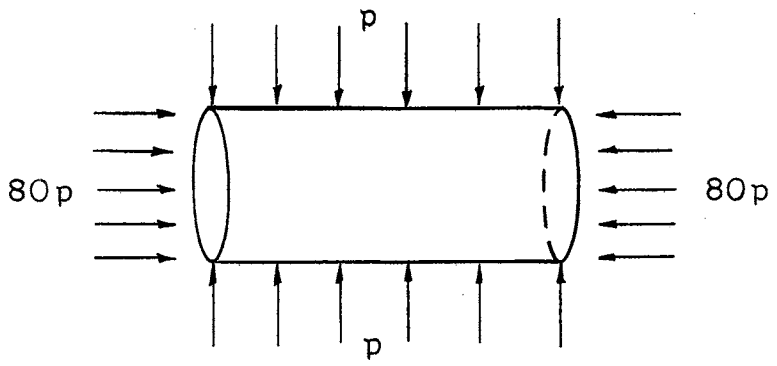

$p^* = \bar{p}E \times 10^{-7}$ psi

		$v_o = w_o = 0$ $v_L = w_L = 0$		$u_L = v_L = w_L = \gamma_L = 0$		$v_o = w_o = 0$ $v_L = w_L = \gamma_L = 0$	
n	m	Finite Element	Flugge	m	Finite Element	m	Finite Element
2	1	1.83	2.14	1	0.467	1	2.03
3	1	0.814	0.894	1	0.69	1	0.89
4	1	1.39	1.47	2	1.01	1	1.39
5	3	1.89	1.93	3	1.25	3	1.92
6	4	2.42	2.37	5	1.43	4	2.37
7	5	2.92	2.86	4	1.57	7	2.69

5.3 Dynamic Instability Without Damping

The boundaries of the regions of dynamic instability when neglecting all damping forces are found by solving equation (95). The first series of problems for which the regions of instability are determined are for cylinders subjected to a pulsating radial pressure and supported in a way such that the following boundary conditions apply:

Boundary Condition	Restrained Displacements
1	$v_o = w_o = v_L = w_L = 0$
2	$u_o = v_o = w_o = u_L = v_L = w_L = 0$
3	$u_o = v_o = w_o = \gamma_o = u_L = v_L = w_L = \gamma_L = 0$
4	$u_o = v_o = w_o = \gamma_o = 0$
5	$w_o = v_L = w_L = \gamma_L = 0$

The boundaries of the regions of instability for each of the boundary conditions given above were calculated and plotted on a non-dimensionalized graph. When plotted in this manner each of these cases gave identical regions which are shown in Figure 15. The region corresponding to $\alpha = 0$ is the same as the solution of the Mathieu differential equation. The regions for $\alpha = 0.6$ and $\alpha = 0.9$ would be the same as the region for $\alpha = 0$ had the frequency of the pulsating load been normalized with respect to the resonant frequency of a shell under a constant load of $0.6\ p^*$ or $0.9\ p^*$ respectively. In that case, θ would have been divided by solutions of equation (93) instead of solutions of equation (91). The values of buckling pres-

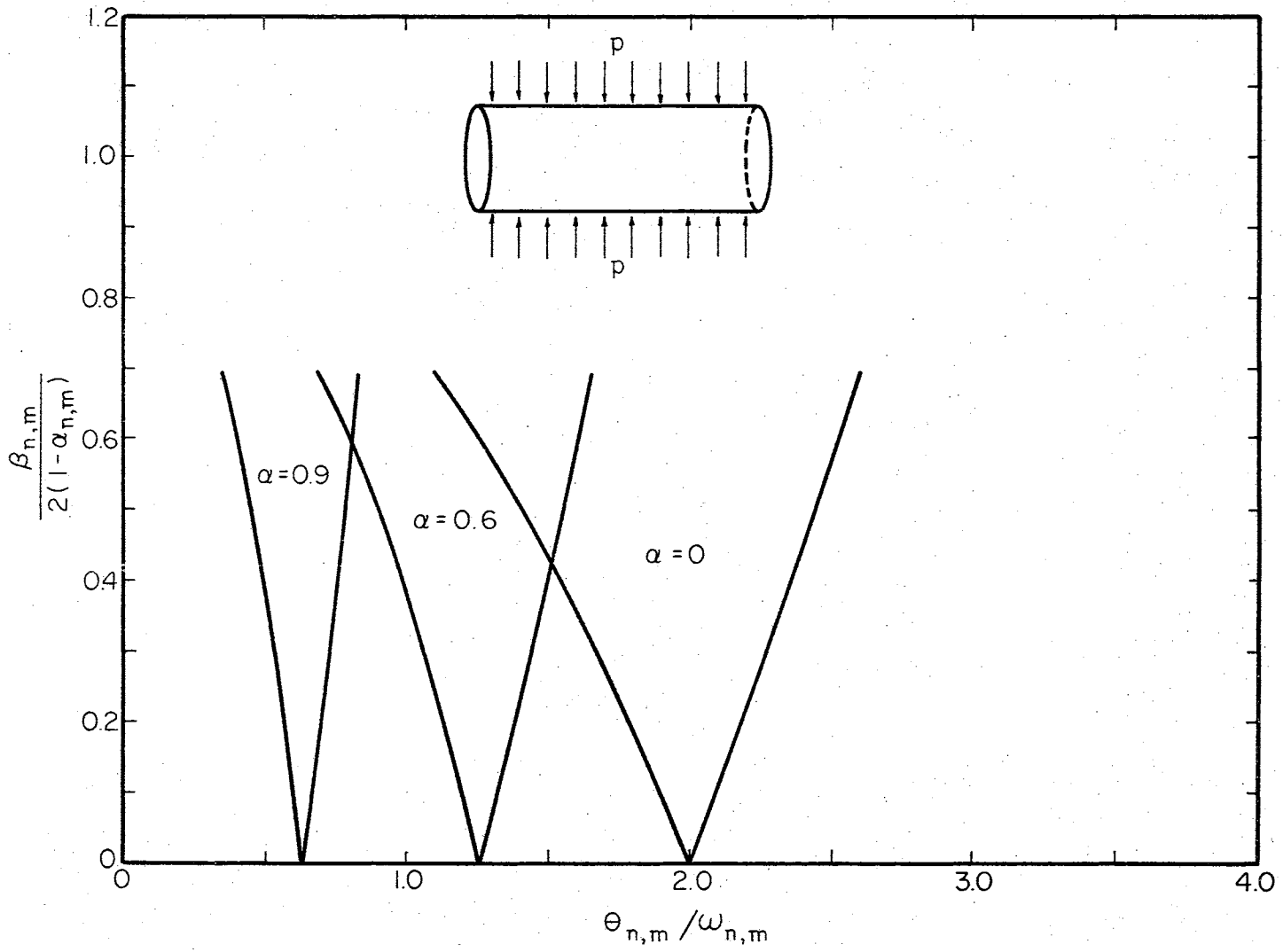

Figure 15. Regions of Dynamic Instability for a Shell Under Uniform Radial Pressure

sures and natural frequencies are given in Table VII and Table VIII, respectively, for several mode shapes for each of the five boundary conditions which were considered. With this information, Figure 15 indicates whether or not a certain load applied at a given frequency will cause dynamic instability of a shell with the assumed dimensions. In each of the preceding cases the mode shapes of buckling and vibration for a given value of n were almost identical; from the most critical values to the least critical values.

The regions of dynamic instability for a shell subjected to a uniform axial pressure and with simply supported ends are shown in Figure 16. The critical axial stress in this cylinder corresponds to a mode shape of $n = 3$ and $m = 1$; therefore, the regions of instability were calculated for $n = 3$. In Figure 17 the regions of dynamic instability are given for the same case except that an additional restraint is imposed in which the ends of the cylinder were not allowed to rotate, i.e., $\gamma = 0$. The critical load occurred in this case for $n = 4$ and $m = 1$. In both of these cases the static buckling and free vibration mode shapes along the axis of the shell were almost identical for equally ranked values, and the regions are the same as these for solutions of the Mathieu equation.

The regions of instability for a shell under axial pressure which is clamped at one end and restrained only in the radial direction at the other end are shown in Figure 18. These regions differ considerably from the previous results, but, in this case, there was a marked difference in the critical mode shapes for buckling and free vibration as shown in Figure 19. The same regions are also shown in Figure 20, in which the frequency of the load, θ, is normalized with respect to

TABLE VII

CRITICAL RADIAL PRESSURES FOR SEVERAL BOUNDARY CONDITIONS

		$p^* = \bar{p}E \times 10^{-7}$ psi						
m	B.C.	n=2	n=3	n=4	n=5	n=6	n=7	n=8
1		3.28	1.07	1.62	2.60	3.86	5.44	
2	1	44.5	4.97	2.35	2.80	3.91	5.37	
3		199	20.8	5.40	3.67	4.28	5.67	
1		13.8	2.11	1.82	2.65	3.88	5.45	7.42
2	2	88.0	10.0	3.37	3.10	4.06	5.54	
3		287	33.3	8.13	4.48	4.58	5.79	7.62
1		13.9	2.12	1.82	2.65	3.88	5.45	7.42
2	3	89.2	10.2	3.40	3.11	4.06	5.54	7.48
3		292	34.1	8.32	4.55	4.61	5.80	7.63
1		0.64	0.83	1.58	2.59	3.87	5.48	
2	4	14.3	2.17	1.83	2.67	3.91	5.50	
3		98.9	10.7	3.49	3.15	4.10	5.60	
1		4.42	1.32	1.69	2.64	3.93	5.58	7.68
2	5	51.1	6.82	2.88	3.01	4.08	5.66	7.72
3		227	29.1	7.97	4.60	4.72	5.99	7.95

TABLE VIII

NATURAL FREQUENCIES FOR SEVERAL
BOUNDARY CONDITIONS

$\omega = \bar{\omega} \sqrt{E/\rho} \times 10^{-5}$ rad/sec

m	B.C.	n=2	n=3	n=4	n=5	n=6	n=7	n=8
1		725	660	1101	1770	2614	3647	
2	1	2676	1431	1339	1844	2645	3664	
3		5723	2974	2067	2133	2765	3723	
1		1491	930	1173	1790	2623	3653	4904
2	2	3790	2057	1624	1951	2688	3685	4921
3		6968	3846	2618	2422	2901	3793	4985
1		1512	940	1176	1792	2623	3653	4904
2	3	3875	2118	1657	1963	2694	3688	4923
3		7189	4039	2754	2498	2937	3812	5000
1		326	582	1089	1765	2612	3641	4835
2	4	1517	934	1175	1793	2625	3652	4903
3		4000	2124	1646	1958	2691	3682	4915
1		810	720	1125	1777	2618	3651	4903
2	5	2760	1592	1441	1887	2664	3674	4915
3		5721	3210	2297	2268	2831	3758	4965

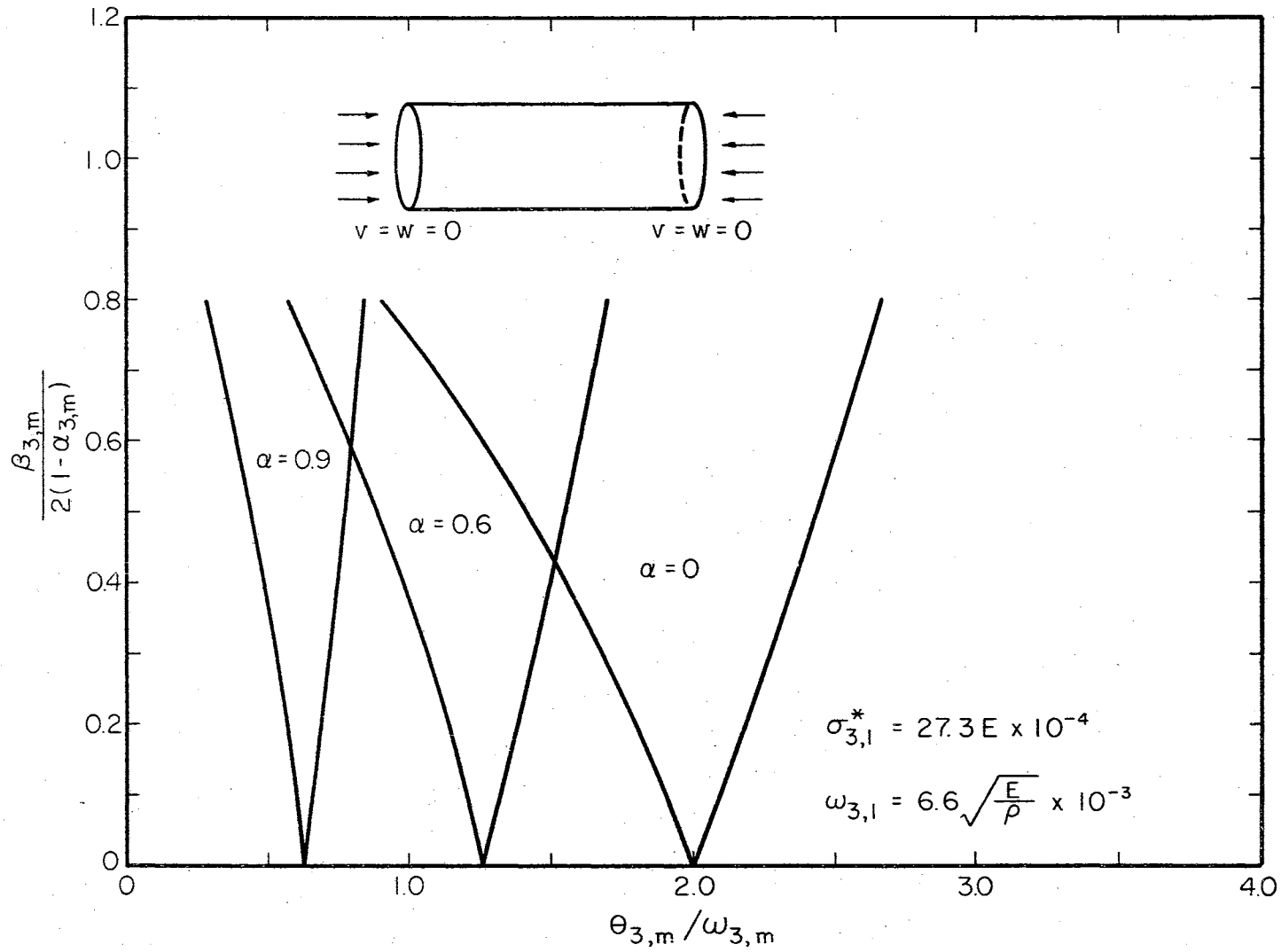

Figure 16. Regions of Dynamic Instability for a Simply Supported Shell Subjected to Axial Pressure

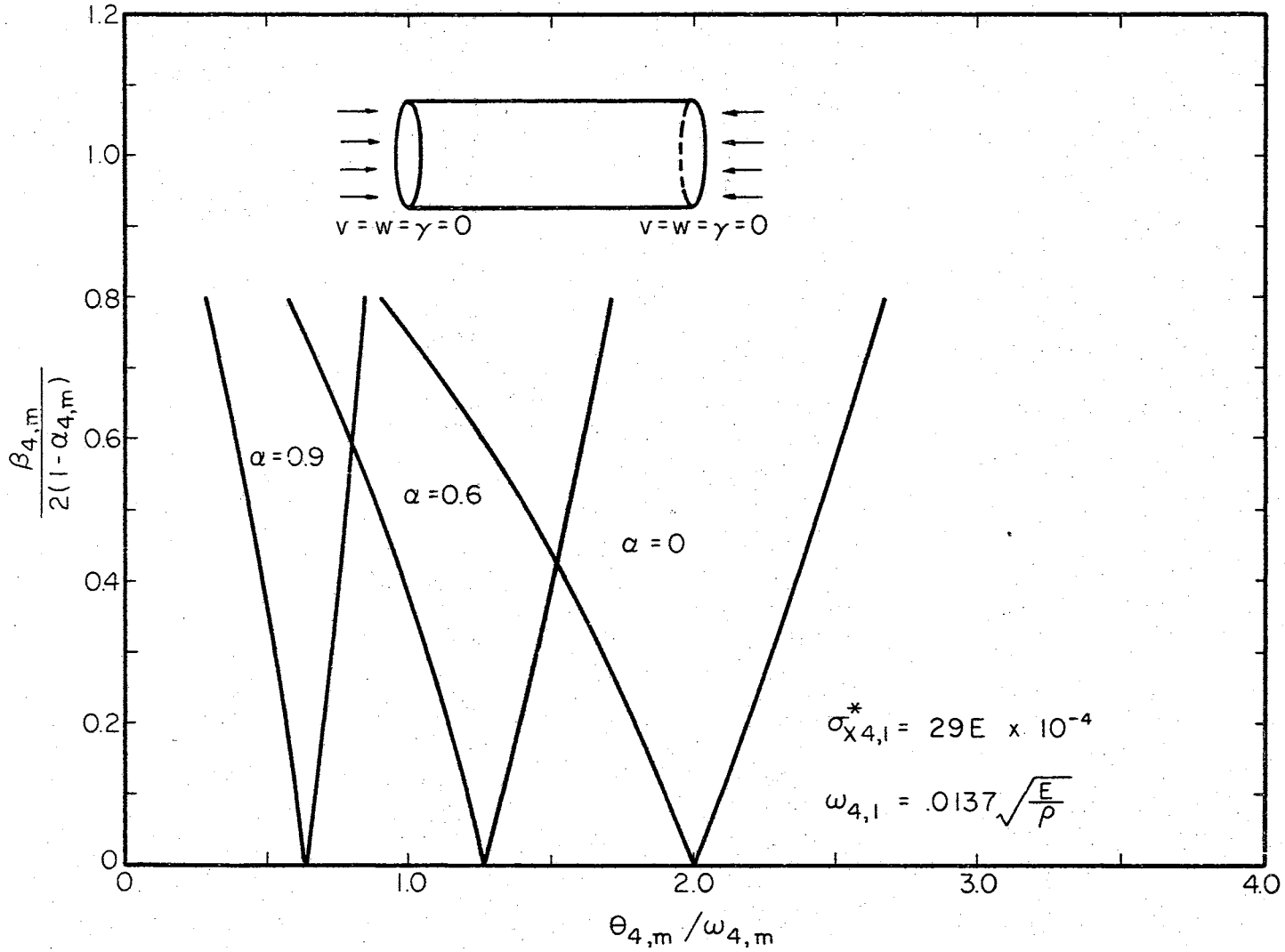

Figure 17. Regions of Dynamic Instability for a Clamped Shell Subjected to Axial Pressure

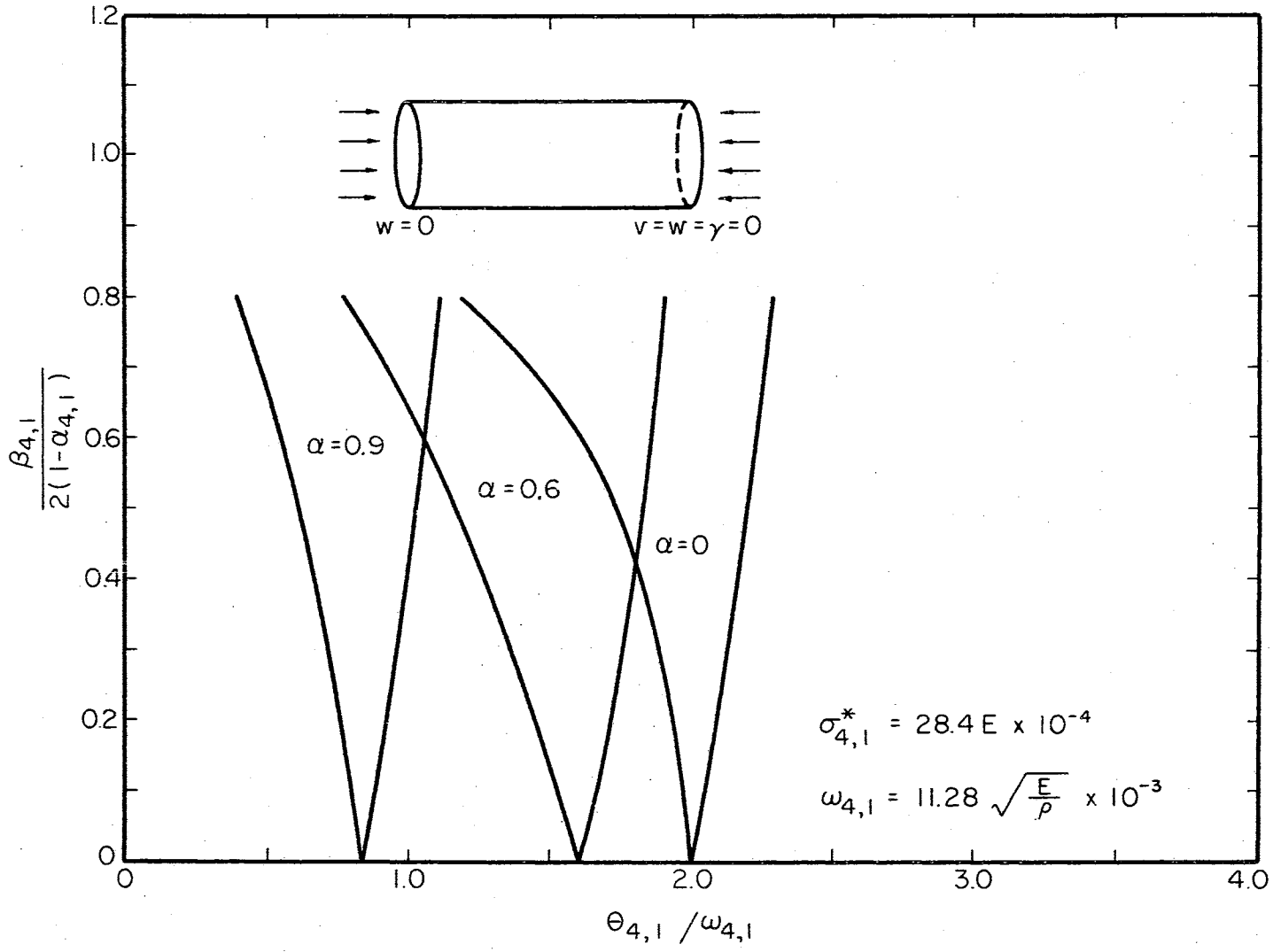

Figure 18. Regions of Dynamic Instability for a Shell Under Axial Load Supported by Boundary Condition Number 5

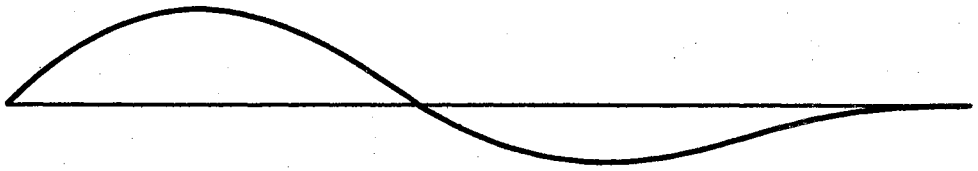

FIRST BUCKLING MODE

FIRST FREE VIBRATION MODE

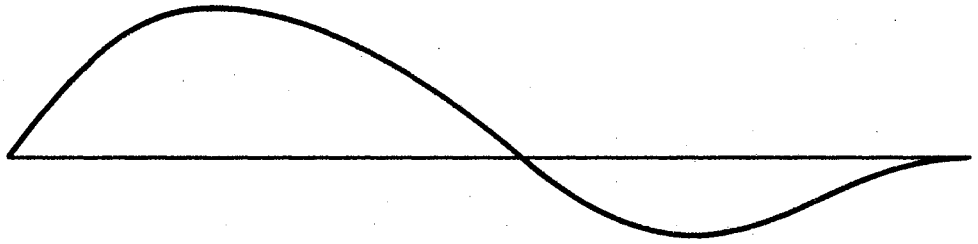

FIRST FREE VIBRATION MODE UNDER
A CONSTANT LOAD $p_o = 0.6p^*$

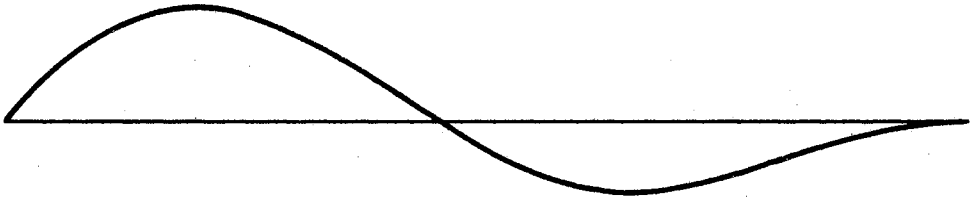

FIRST FREE VIBRATION MODE UNDER
A CONTANT LOAD $p_o = 0.9p^*$

Figure 19. Mode Shapes for a Shell Under Axial Load Supported by Boundary Condition Number 5

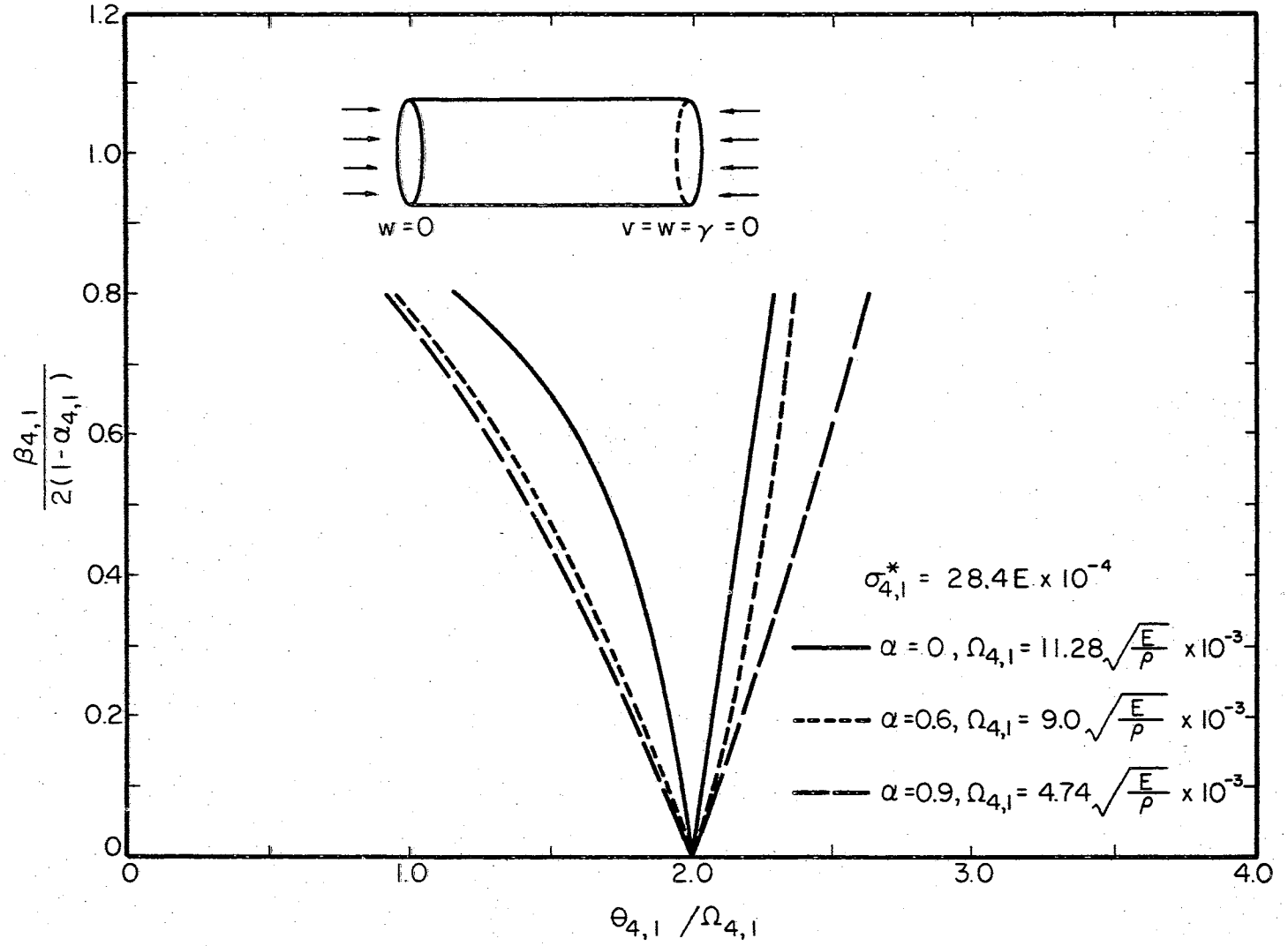

Figure 20. Regions of Dynamic Instability Normalized by Ω

the resonant frequency of vibration under the respective values of constant load, Ω, instead of the natural frequency, ω. The regions corresponding to $\alpha = .6$ and $\alpha = .9$ when plotted in this manner correspond closely to the region for $\alpha = 0$ in the previous examples, but the buckling and vibration mode shapes are similar for these values of the constant load as shown in Figure 19.

The regions of instability for a cantilevered shell under a uniform axial load are given in Figure 21. The regions for this case are slightly narrower than the regions given by solutions of the Mathieu equation. The mode shapes for static buckling and free vibration shown in Figure 22 differ slightly. In the previous example a large difference in the buckling and vibration mode shapes resulted in a large difference in the regions of instability and in this example a small variation in the mode shapes produced a small change from the regions of unbounded solutions of Mathieu equation. This trend was also observed by Brown (30) and Hutt (31) for the dynamic stability of rods and plates. Hutt (31) offered an explanation for this occurrence for the dynamic stability of plates.

Figures 23, 24, and 25 give the principal regions of dynamic instability for a shell subjected to combined axial and radial pressure for three support conditions. The mode shapes for static buckling and free vibration are similar for each of these conditions and the resulting regions of instability are solutions of the Mathieu equation.

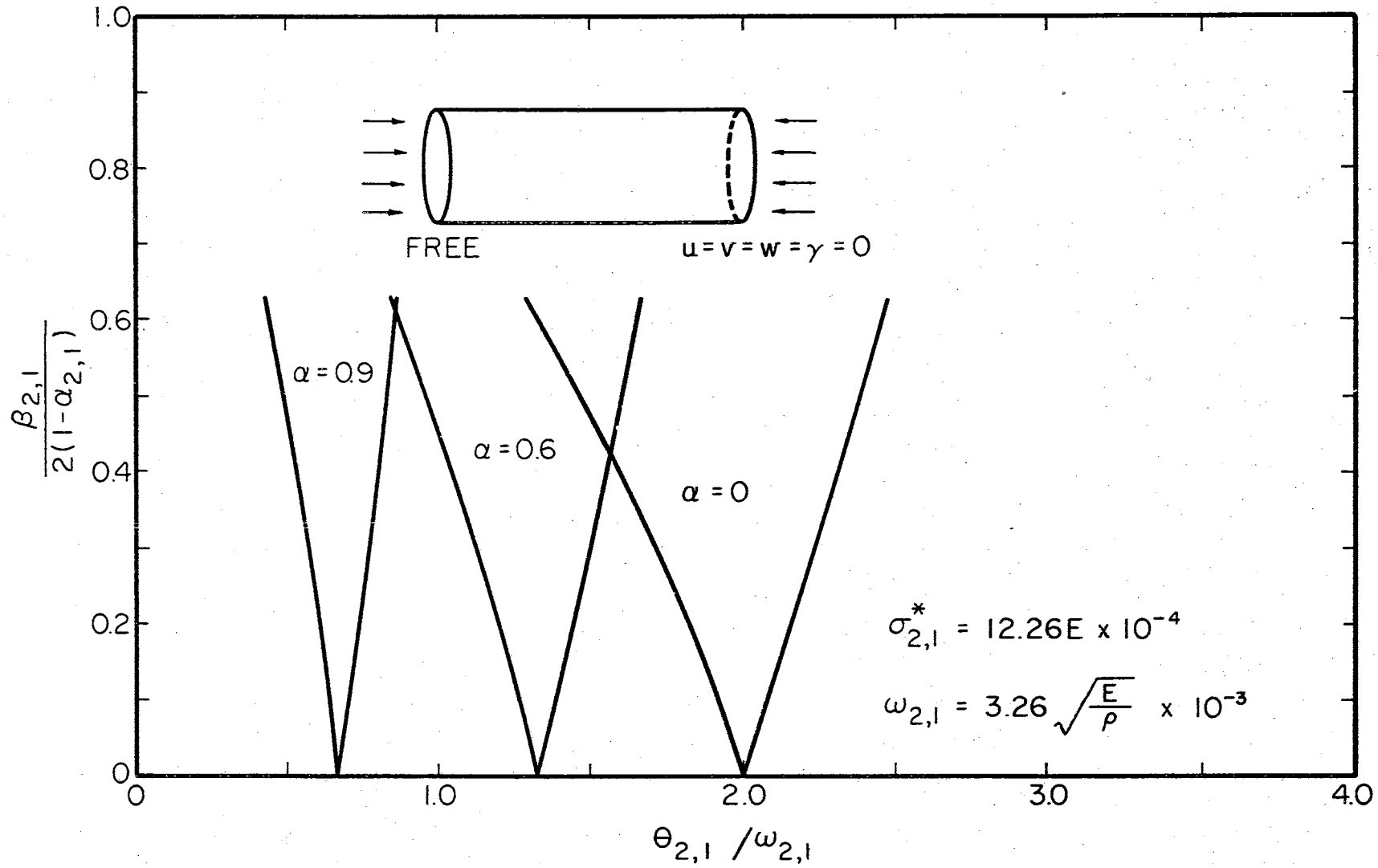

Figure 21. Regions of Dynamic Instability of a Cantilevered Shell Under Axial Pressure

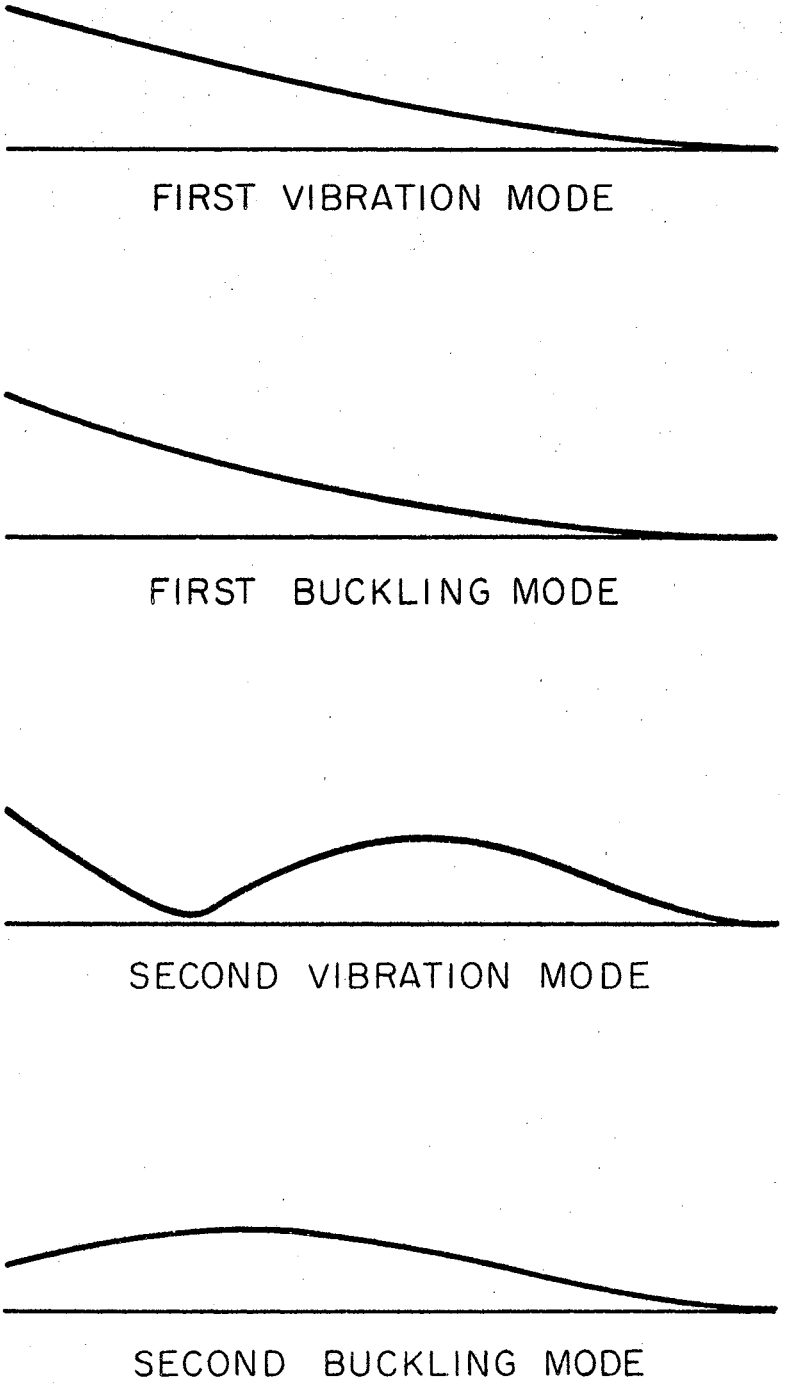

Figure 22. Mode Shapes for a Cantilevered Shell Under Axial Load

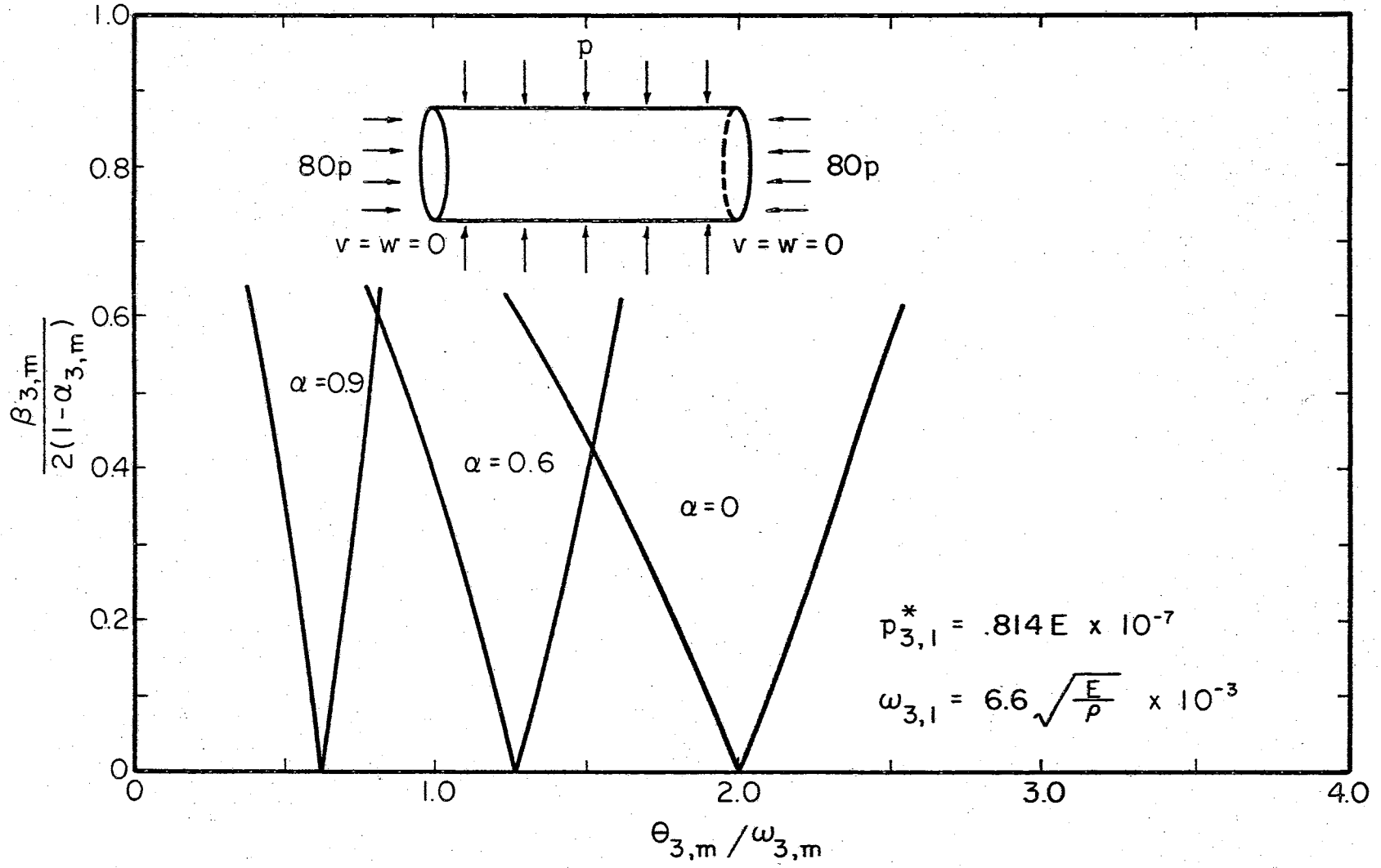

Figure 23. Regions of Dynamic Instability for a Simply Supported Shell Subjected to Combined Loading

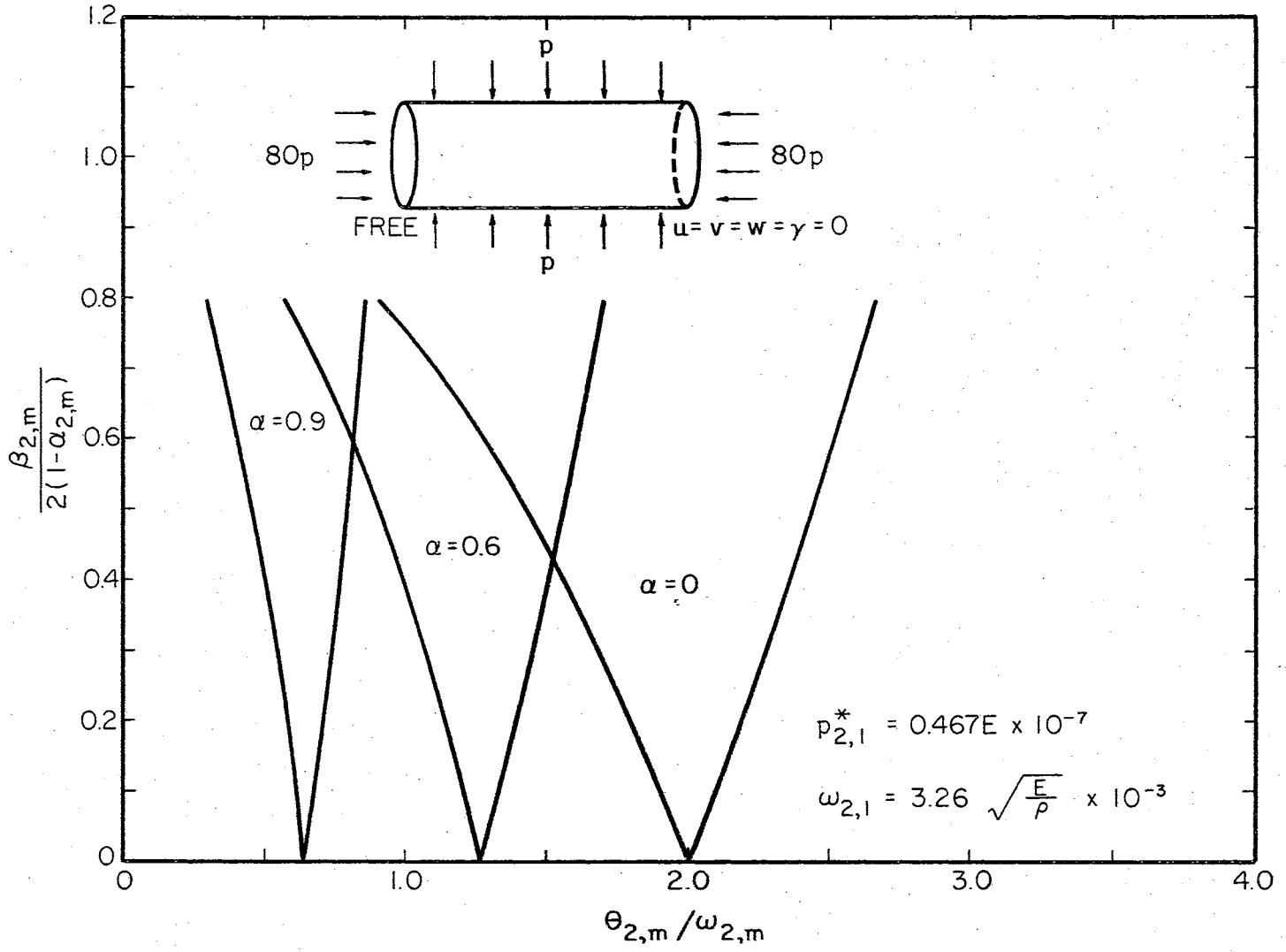

Figure 24. Regions of Dynamic Instability for a Cantilevered Shell Under Combined Pressure

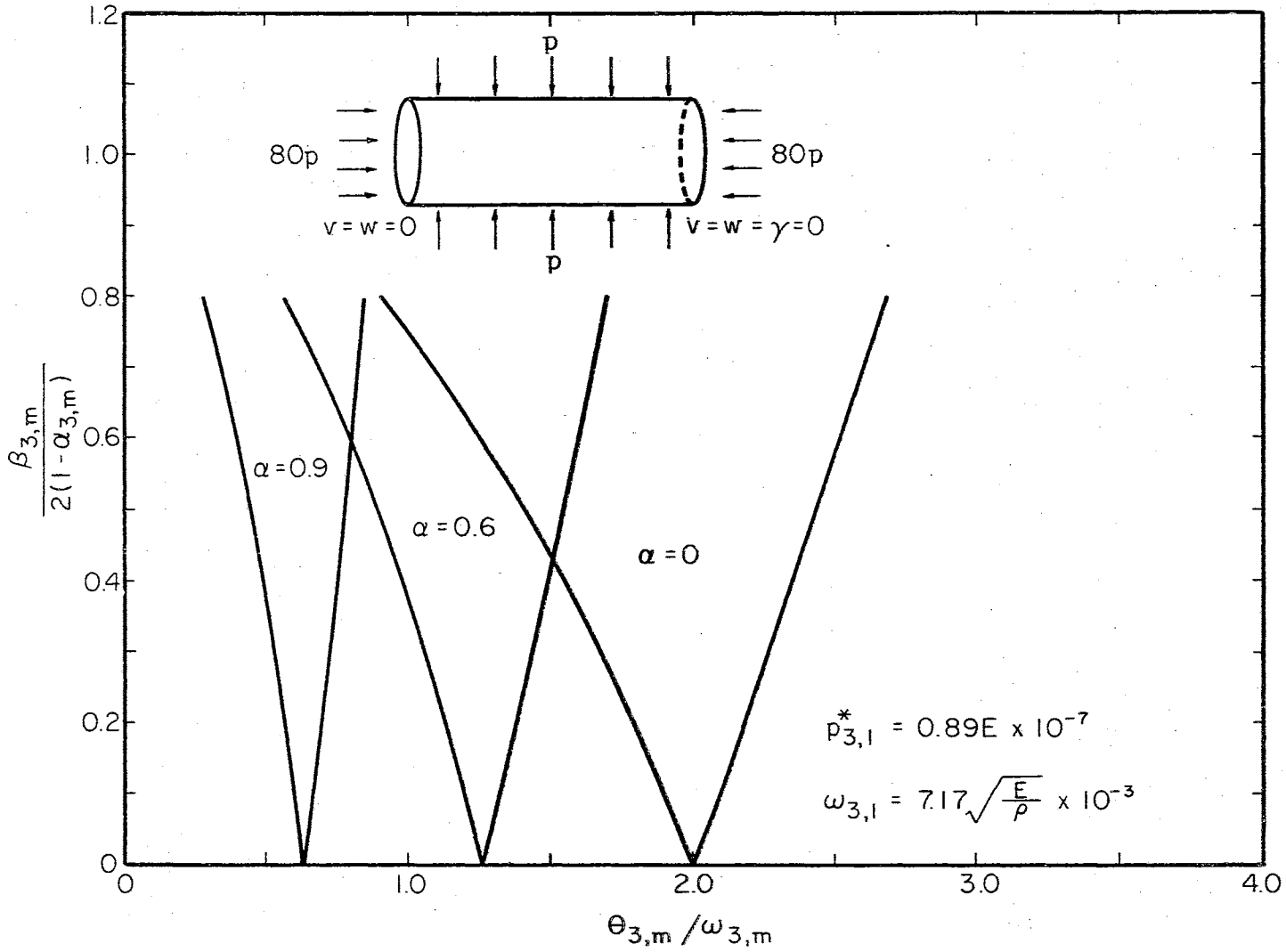

Figure 25. Regions of Dynamic Instability for a Clamped-Simply Supported Shell Subjected to Combined Loading

5.4 Dynamic Instability With Damping

The three examples presented in the previous section with combined loading were also solved including damping forces and the resulting regions are shown in Figures 26, 27, and 28. The parameter, η, which is used as a measure of the damping force is defined by the following relation:

$$\eta = \frac{c}{\omega \rho h} \tag{99}$$

in which

c = damping coefficient

ω = natural frequency of the shell

ρ = mass density per unit volume of the material

h = thickness of the shell.

The effect that the damping forces have on the regions of instability is to require that the load must have a finite value to cause dynamic instability. Also, the presence of damping produces narrower instability regions. In the cases given for $\eta = 0.1$ and $\alpha = 0$ the periodic load must be greater than four-tenths of the static buckling load to be capable of causing dynamic instability.

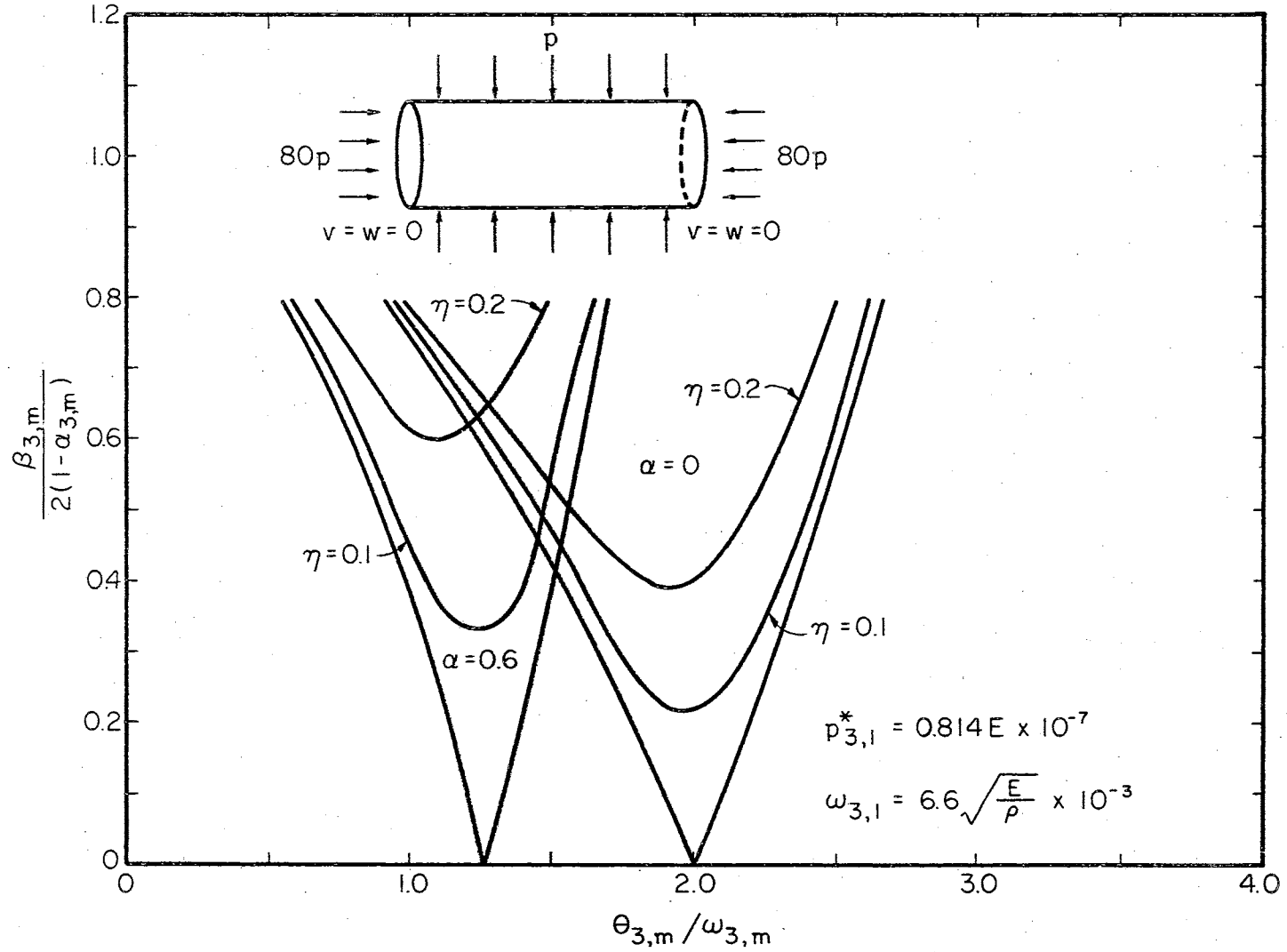

Figure 26. Regions of Dynamic Instability of a Simply Supported Shell Including Damping

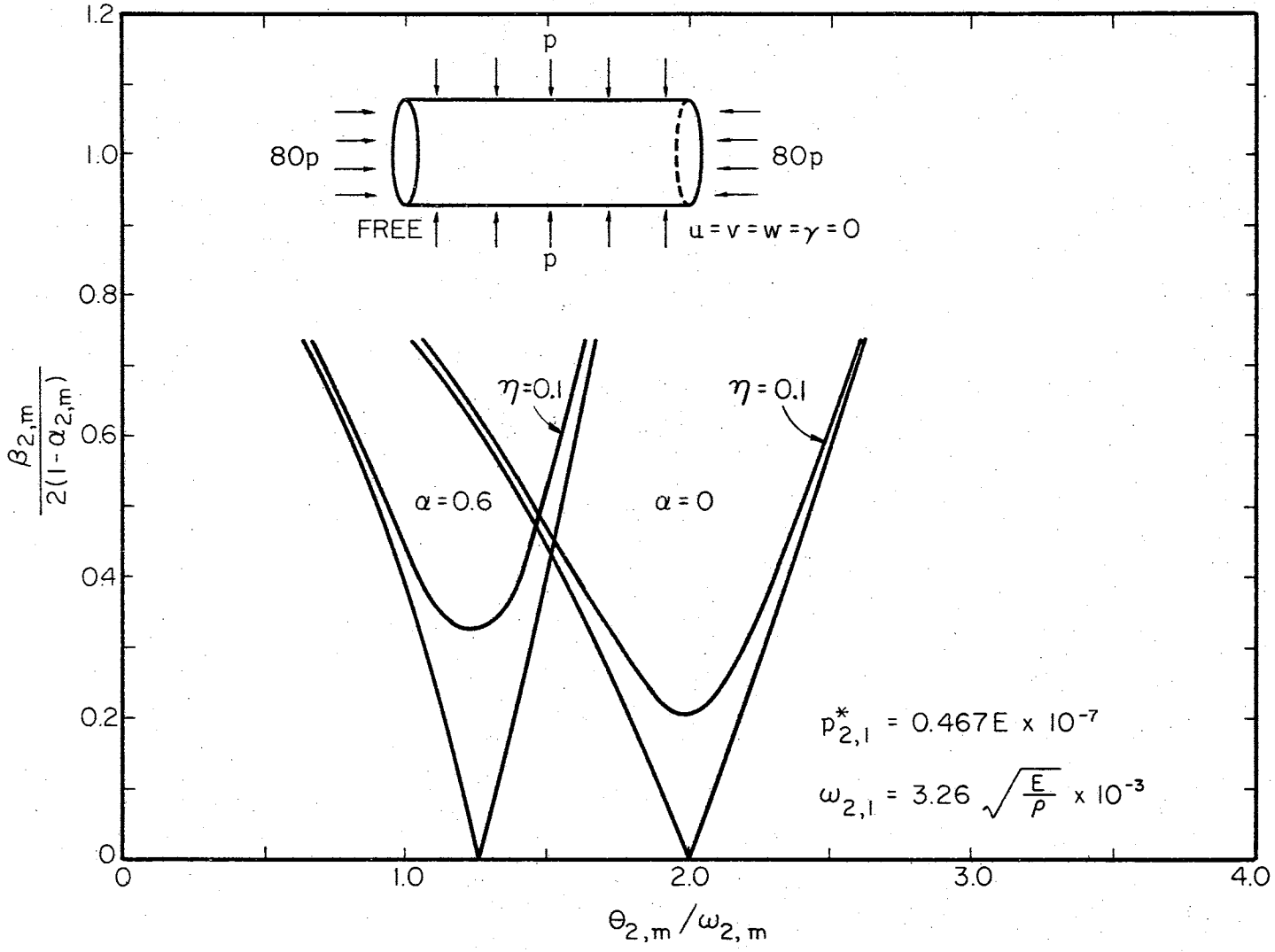

Figure 27. Regions of Dynamic Instability of a Cantilevered Shell Including Damping

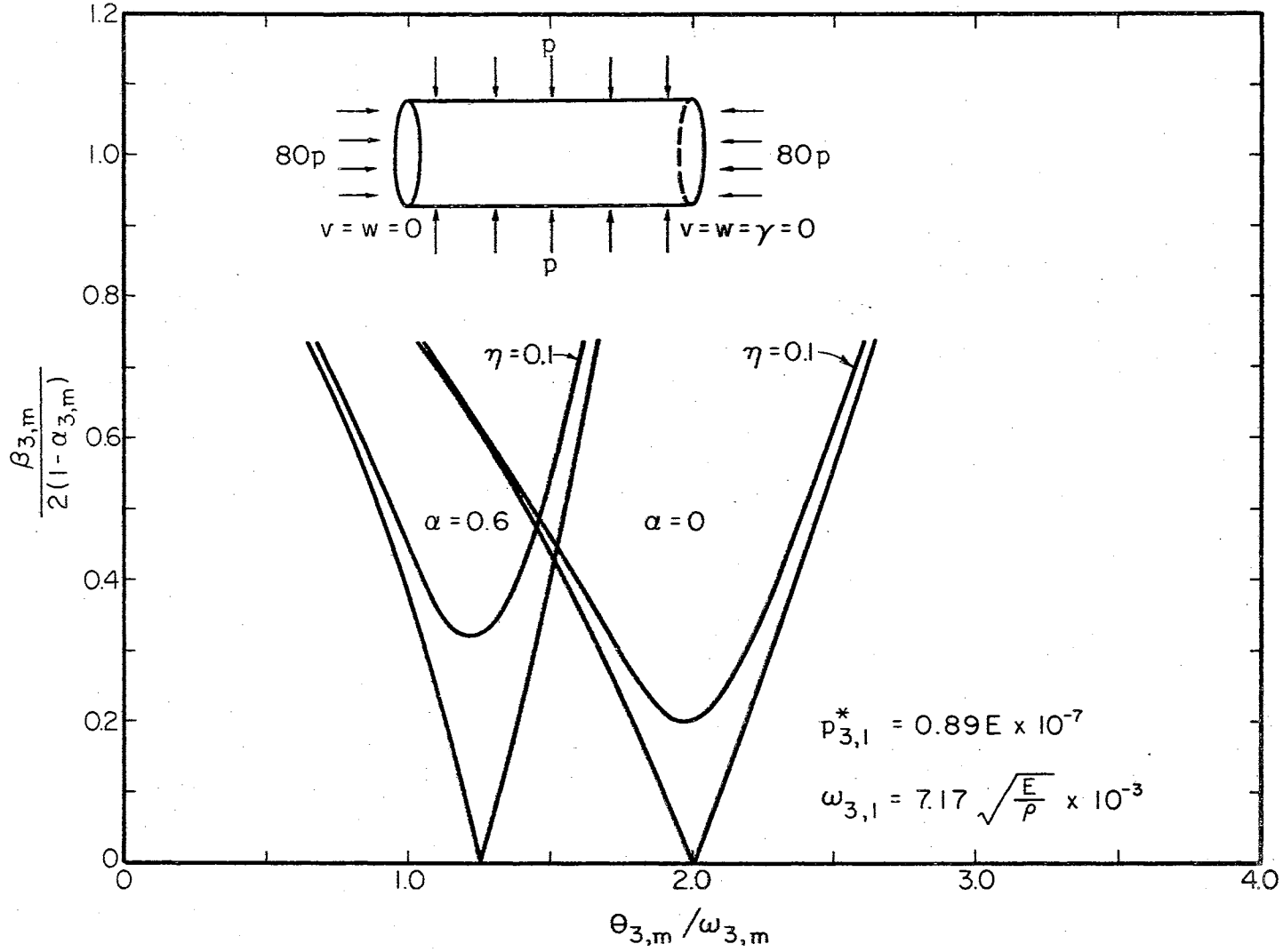

Figure 28. Regions of Dynamic Instability of a Clamped-Simply Supported Shell Including Damping

CHAPTER VI

SUMMARY AND CONCLUSIONS

6.1 Summary and Conclusions

A method for determining the principal regions of dynamic instability for cylindrical shells has been developed in this thesis using a stiffness formulation of the finite element method. The equations of motion of a shell element were derived from Hamilton's principle. The equations of the boundaries of the regions of dynamic instability were derived from certain periodic solutions of the equations of motion. The stiffness matrices were obtained by assuming a displacement field throughout the element. The accuracy of this approach was improved by assuming a displacement field which had more arbitrary constants than the number of degrees of freedom of the element and using the principle of minimum potential energy to express the dependent constants in terms of the independent constants. This procedure gave overall results which compared better with existing solutions for static buckling and free vibration with a fewer number of elements than the standard procedure. If a further improvement is desired in the accuracy of this method then, more exact strain-displacement relations should be assumed in deriving the stiffness matrix. A shell subjected to several boundary conditions and different combinations of axial and radial pressure was analyzed. The effect of damping was included in some of the examples.

The similarity of the mode shapes for static buckling and free vibration was found to have a direct influence on the regions of instability. In all cases in which these mode shapes were identical the resulting regions were the same as those given in Figure 15. In those cases in which the mode shapes differed the resulting regions of instability differed from those in Figure 15.

The finite element method makes the solution of the dynamic stability problem of cylindrical shells feasible. Other approaches to this problem are extremely difficult. The ease with which various boundary conditions can be applied is a primary advantage of the method. Support conditions which have not been solved by other methods are easily handled with the finite element technique.

6.2 Extension of Work

The examples which were solved in this thesis were restricted to cylindrical shells subjected to a uniformly distributed axial and radial pressure. The shell is assumed to be initially perfect and constructed of a homogeneous, isotropic, and linearly elastic material. The method could be readily adapted to anisotropic and multilayered shells. Other loading conditions such as a torque applied about the axis of the cylinder could also be considered. The buckling of a shell under axial pressure should be investigated by taking small initial imperfections of the shape of the cylinder into account. Shells of revolution could be considered by using a conical frusta for a finite element. An investigation to establish some criteria for the optimum displacement function should be conducted.

BIBLIOGRAPHY

(1) Rayleigh, John William Strutt (Lord), The Theory of Sound. The Macmillian Co., Ltd., London, 1926.

(2) Beilin, E. A. and G. U. Dzhanelidze, "Survey of the Works on the Dynamic Stability of Elastic Systems." Prikl. Mat. i Mekhan., Vol. 16, No. 5, 1952, pp. 635-648. (Available in English as ASTIA No. AD-264148.)

(3) Beliaev, N. M., "Stability of Prismatic Rods Subjected to Variable Longitudinal Forces." Collection of Papers: Engineering Construction and Structural Mechanics, Leningrad, 1924.

(4) Krylov, N. M. and H. N. Bogoliukov, "An Investigation of the Appearance of Resonance of the Transverse Vibrations of Rods Due to the Action of Normal Periodic Forces on an End." Investigation of Vibrations of Structures, (ONTI Karkov/Kiev, 1935), pp. 25-42.

(5) Bodner, V. A., "The Stability of Plates Subjected to Longitudinal Periodic Forces." Prikl. Mat. i Mekhan., (N.S.) Vol. 2, 1938, pp. 87-104.

(6) Khalilov, Z. I., "The Dynamic Stability of a Plate Under the Action of Periodic Longitudinal Forces." Tr. Azerb. Gos. Univ., Ser. Mar., Vol. 1, 1942, pp. 28-32.

(7) Einaudi, R., "Sulle Configurazioni di Equilibrio Instable di una Piastra Sollecitata da Sforzi Tangenziali Pulsanti." Atti. Accad. Gioenia, Vol. 1, Memoria XX, 1935-36, pp. 1-5.

(8) Ambartsumian, S. A. and A. A. Khachatrian, "On the Stability and Vibrations of Anisotropic Plates." Izv. Akad. Nauk, SSSR, Otd. Tekhn. Nauk. Mekhan. i Mashinostr., Vol. 1, 1960, pp. 113-122.

(9) Dzhanelidze, G. U. and M. A. Radtsig, "Dynamic Stability of Rings Subjected to Normal Periodic Forces." Prikel. Mat. i Mekhan., (N. S.) Vol. 4, 1940, pp. 55-60.

(10) Markov, A. N., "The Dynamic Stability of Anisotropic Cylindrical Shells." Prikl. Mat. i Mekhan., Vol. 13, 1949, pp. 145-150. (Available in English as TM-43, Douglas Aircraft Company, Santa Monica, California.)

(11) Bolotin, V. V., "Stability of a Thin-Walled Spherical Shell Subjected to a Periodic Pressure." Collection of Papers: Design for Stability. Vol. 2, pp. 284-289, Moscow, 1958.

(12) Federhofer, Karl, "Die durch pulsierende Axialkrafte gedruckte Kreiszylindershale." Oesterr. Akad, Wiss., Math. Naturw. Vol. 163, 1954, pp. 41-54.

(13) Bublik, B. M. and V. I. Merkulov, "On the Dynamic Stability of a Thin Elastic Shell Filled with a Liquid." Prikl. Mat. i Mekhan. Vol. 24, 1960, pp. 941-947.

(14) Mettler, E., "Biegeschwingungen eines Stabes mit kleiner Vorkrummung, exzentrisch angreifender publsierender Axiallast und statischer Querbelastung." Forshungshefte aus d. Geb. d. Stahlbaues, Vol. 4, 1941, pp. 1-23.

(15) Naumov, K. A., "The Stability of Prismatic Rods Allowing for Damping." Tr. Mosk. Inst. Inzh. Transp., Vol. 69, 1946, pp. 132-141.

(16) Bolotin, V. V., Dynamic Stability of Elastic Systems. Holden-Day, Inc., San Francisco, 1964.

(17) Wood, J. D. and L. R. Koval, "Buckling of Cylindrical Shells under Dynamic Loads." Amer. Inst. Aero. Astro. Jour., Vol. 1, 1963, pp. 2576-2582.

(18) Bieniek, M. P., T. C. Fan, and L. M. Lackman, "Dynamic Stability of Cylindrical Shells." Amer. Inst. Aero. Astro. Jour., Vol. 4, 1966, pp. 495-500.

(19) Agamirov, V. L. and A. S. Vol'mir, "Behavior of a Cylindrical Shell Subject to the Dynamic Loadings of Pressure Around the Circumference." Akad. Nauk, SSSR Investia, Vol. 1, No. 3, 1959, pp. 78-83.

(20) Vol'mir, A. S., "Stability of Cylindrical Shells Subject to Dynamic Loading." Doklady Akad. Nauk SSSR, Vol. 123, 1958, pp, 806-808.

(21) Brachkovski, B. Z., "On the Dynamic Stability of Elastic Systems." Prikl. Mat. i Mekhan. (N. S.) Vol. 6, 1942, pp. 87-88.

(22) Bolotin, V. V., "On the Parametric Excitation of Transverse Vibrations." Collection of Papers: Transverse Vibrations and Critical Velocities. Akademiia Nauk SSSR, Moscow, 1953.

(23) Turner, M. J., R. W. Clough, H. C. Martin, and L. J. Topp, "Stiffness and Deflection Analysis of Complex Structures." Jour. Aero. Sciences, Vol. 23, No. 9, 1956, pp. 805-823.

(24) Melosh, R. J. "Basis for Derivation of Matrices for the Direct Stiffness Method." Amer. Inst. Aero. Astro. Jour., Vol. 1, No. 7, 1963, pp. 1631-1637.

(25) Best, G. C., "A General Formula for Stiffness Matrices of Structural Elements." Amer. Inst. Aero. Astro. Jour., Vol. 1, No. 8, 1963, pp. 1920-1921.

(26) Pian, T. H. H., "Derivation of Element Stiffness Matrices." Amer. Inst. Aero. Astro. Jour., Tech. Notes, Vol. 2, 1964, pp. 576-577.

(27) Zienkiewicz, O. C., and T. K. Cheung, "The Finite Element Method for Analysis of Elastic Isotropic and Orthotropic Slabs." Proc. Instn. Civ. Engrs., Vol. 28, 1964, pp. 471-488.

(28) Severn, R. T. and P. R. Taylor, "The Finite Element Method for Flexure of Slabs when Stress Distributions are Assumed." Proc. Instn. Civ. Engrs., Vol. 34, 1966, pp. 153-170.

(29) Percy, J. H., T. H. H. Pian, S. Klein, and D. R. Navaratna, "Application of Matrix Displacement Method to Linear Elastic Analysis of Shells of Revolution." Amer. Inst. Aero. Astro. Jour., Vol. 3, 1965, pp. 2138-2145.

(30) Connor, J. J. and C. Brebbia, "Stiffness Matrix for Shallow Rectangular Shell Element." Proc. Amer. Soc. Civ. Engrs., Engr. Mech. Jour., Oct. 1967, pp. 43-65.

(31) Webster, J. J., "Free Vibrations of Shells of Revolution Using Ring Finite Elements." Int. Jour. Mech. Sci., Vol. 9, 1967, pp. 559-570.

(32) Brown, John E., "Dynamic Stability of Bars by the Finite Element Method." Master's Report, Oklahoma State University, Stillwater, Oklahoma, 1968.

(33) Hutt, J. M., "Dynamic Stability of Plates by Finite Elements." Ph.D. Thesis, Oklahoma State University, Stillwater, Oklahoma, 1968.

(34) Goldstein, H., Classical Mechanics. Addison-Wesley Press Inc., Cambridge, 1950.

(35) Greenwood, D. T., Principles of Dynamics. Prentice-Hall, Englewood Cliffs, 1965.

(36) Timoshenko, S., and S. Woinowsky-Krieger, Theory of Plates and Shells. 2nd Ed. McGraw-Hill Book Co., Inc., New York, 1959.

(37) Kraus, H., Thin Elastic Shells. John Wiley and Sons, Inc., New York, 1967.

(38) Arnold, R. N., and G. B. Warburton, "Flexural Vibrations of the Walls of Thin Cylindrical Shells Having Freely Supported Ends." Proc. Roy. Soc. (London), Ser. A, Vol. 197, 1949, pp. 238-256.

(39) Flugge, W., Stresses in Shells. Springer-Verlag, New York, 1966.

VITA

Delvin Errol Black

Candidate for the Degree of

Doctor of Philosophy

Thesis: DYNAMIC STABILITY OF CYLINDRICAL SHELLS BY FINITE ELEMENTS

Major Field: Civil Engineering

Biographical:

Personal Data: Born at Wellington, Texas, December 11, 1940, the son of Osa and Marie Black.

Education: Attended grade school at Quail, Texas, and Wellington, Texas; graduated from Arnett High School near Hollis, Oklahoma in 1959; received the Bachelor of Science degree in Civil Engineering from Oklahoma State University, Stillwater, Oklahoma, in May, 1964; received the Master of Science degree in Civil Engineering in May, 1965, from Oklahoma State University; completed the requirements for the Doctor of Philosophy degree in May, 1968.

Professional Experience: Graduate teaching assistant in the school of Civil Engineering, Oklahoma State University, 1967-1968.